STUDY OF SQUEEZE ACTION DAMPING OF GAS FILM

by

Shoichi Yamanami

B.S. in M.E., University of Tokyo, March 1954

SUBMITTED IN PARTIAL FULFILLMENT OF
THE REQUIREMENTS FOR THE DEGREE OF

MASTER OF SCIENCE IN MECHANICAL ENGINEERING

at the

MASSACHUSETTS INSTITUTE OF TECHNOLOGY

MAY, 1962

Signature of Author_____
Department of Mechanical Engineering, May 15, 19

Certified by_____
Thesis Supervisor

Accepted by_____
Chairman, Departmental Committee on Graduate Students

STUDY OF SQUEEZE ACTION DAMPING OF GAS FILM

by

SHOICHI YAMANAMI

Submitted to the Department of Mechanical Engineering of the Massachusetts Institute of Technology on May 15, 1962

ABSTRACT

The transient pressure distribution in squeeze gas film contained between two parallel surfaces moving in the normal direction in absence of tangential motion was studied. An analytical approach was attempted, particularly in two cases where the boundaries of the gas film were circular and annular, with the following assumptions. The thickness of the gas film was assumed to be sufficiently thin so that the temperature of the gas film might approximately keep constant because of its rapid heat conduction. In addition the motion of the surfaces was assumed to be a periodic motion of a small amplitude in comparison with the thickness of the gas film. Furthermore, the flow of the film gas was considered to be a creeping flow where the inertia term is negligible compared with its viscosity term. This analysis was investigated by experiment where the pressure distribution was measured in terms of damping ratio. The agreement between the predicted values and those obtained by experiment was considerably good.

Thesis Supervisor: Herbert H. Richardson

Title: Associate Professor of Mechanical Engineering

ACKNOWLEDGEMENTS

I would like to thank Professor Richardson for his encouragement and assistance in writing this thesis. I would also like to thank Mr. Williams Griffin for his assistance in creating an environment conducive to a high level of scholarly research. I would also like to thank Miss R. Sanzotta for her help in editing this thesis.

This thesis was supported in part by the U. S. Air Force, (ASD), under contract AF 33(657)-7535 and sponsored by the Division of Sponsored Research of Massachusetts Institute of Technology.

TABLE OF CONTENTS

LIST OF FIGURES

LIST OF FIGURES (CONTINUED)

LIST OF FIGURES (CONTINUED)

INTRODUCTION

A thin gas film bounded by two parallel surfaces will have a transient pressure distribution when it is squeezed by the motion of the surfaces in normal direction. This phenomenon implies the possibility for this type of mechanical device to provide an appropriate damping with various kinds of dynamic systems, for instance, value spools, torque motors, hot gas gyros, etc.

Although there are quite a few papers related to the study of squeeze gas films, the dynamic behavior has still remained for the most part, to be of interest.

The object of this paper is focused on a theoretical approach to analize the transient pressure distribution produced by the squeezing action of the surfaces bounding the gas film in absence of tangential motion, particularly concerning the cases of both circular and annular boundary.

The exact solution of this kind of problem seems impossible as far as the present mathematical methods are concerned. However, it is practicable to use some assumptions to simplify the problem. As is shown in a recent paper by Langlois (Reference 2), the assumption that the flow of the film gas caused by squeezing action is a creeping flow where inertia term can be neglected in comparison with viscosity term, and the gas is subjected to isothermal change with constant viscosity, reduces the governing equation of the pressure distribution of the gas film to the following expression:

$$\frac{\partial}{\partial X}\left(h^3\frac{\partial p2}{\partial X}\right)+\frac{\partial}{\partial y}\left(h^3\frac{\partial p2}{\partial y}\right)=24\mu\,\frac{\partial(ph)}{\partial t} \qquad (1)$$

h: thickness of gas film

p: pressure of gas film

μ: viscosity of film gas

t: time

If the boundary surfaces are rigid enough and the squeeze action is of parallel motion in absence of both tangential and rotational motion, the thickness of the film h will be represented by a function of time only. In this case, equation (1) becomes

$$\nabla^2 p^2 = \frac{24}{h^3} \mu \frac{\partial}{\partial t} (ph) \qquad (2)$$

Michael (Reference 3) has recently developed equation (1) to obtain the solution of rectangular boundary plates where the motion of the plates contains rotation too. It is one of the routine approaches to linearize such equations like (1) to employ perturbation method. To establish equation (1), the flow of the film gas has been assumed to be subjected to isothermal process. It seems to be contradiction because squeeze action will give change to the temperature of the gas film. However, if the thickness of the gas film is sufficiently thin and the ambient material can be considered to be a semi-infinite body of high thermal conductivity, the isothermal assumption will be preserved in safety. Furthermore, if the thickness is sufficiently thin, Reynolds' number will become small which makes the assumption of creeping flow hold. In this paper, the step change of the temperature of the gas film is discussed to investigate the isothermal assumption, and also Reynolds' number is calculated with some approximation. To solve equation (2) regarding annular and circular boundaries by introducing small perturbation method to linearize it will end up with an ordinary type of differential equation which is often seen in diffusion problems.

THEORETICAL ANALYSIS

The representation of equation (2) in cylindrical coordinates reads:

$$\frac{1}{r}\frac{\partial}{\partial r}\left[r\frac{\partial}{\partial r}(p^2)\right] = \frac{24}{h^3}\mu\frac{\partial}{\partial t}(ph) \tag{3}$$

By employing perturbation method, which is expressed by

$$h(t) = h_o + \delta h(t); \quad \left(\frac{\delta h}{h_o} \ll 1\right) \tag{4}$$

$$p(r,t) = p_o + \delta p(r,t); \quad \left(\frac{\delta p}{p_o} \ll 1\right) \tag{5}$$

h_o: neutral thickness of gas film

p_o: ambient pressure

equation (3) can be written as follows:

$$\frac{1}{r}\frac{\partial}{\partial}\left(r\frac{\partial \delta p}{\partial r}\right) = \frac{12\mu}{h_o^2}\frac{\partial}{\partial t}\left(\frac{\delta p}{p_o}+\frac{\delta h}{h_o}\right) \tag{6}$$

The normalized representation of equation (6) is given by:

$$\frac{1}{R}\frac{\partial}{\partial R}\left(R\frac{\partial \underline{P}}{\partial R}\right) = a\frac{\partial}{\partial \textcircled{H}}(\underline{P} + H) \tag{7}$$

$R = r/r_o$

$\underline{P} = \delta p/p_o$

$H = \delta h/h_o$

$\textcircled{H} = wt$

$a = \dfrac{12\mu\, r_o^2 w}{h_o^2 p_o}$

r_o = outer radius of boundary

Circular Boundary

Boundary conditions for circular case are:

$$\underline{P}\ (1, \textcircled{H}) = 0$$

$$\underline{P}\ (0, \textcircled{H}) = \text{Finite}$$

If the motion of the surfaces is step function, the derivative of H with respect to time becomes zero. In addition, the initial pressure distribution of the gas film may be uniform which is approximately proportional to the change of volume of the gas film provided that the thermal diffusibility is sufficiently fast to assume an isothermal change; i.e.

$$\frac{\partial H}{\partial t}_{\text{step}} = 0$$

$$\underline{P}\ (R.0) = \underline{P}_s$$

With these conditions, equation (7) can be solved by the method of separation of variables which gives the following solution:

$$\underline{P} = \sum_{n=1}^{\infty} \frac{2P_s\, e^{-\frac{\partial n^2}{a}\textcircled{H}}}{\partial n J_1(\partial n)} J_0(\partial n R) \qquad (8)$$

where $J_0\ (\partial_n) = 0$ (9)

Therefore, the force F(r.t) exerted on the surfaces can be calculated by integrating the pressure $(p-p_o)$ with respect to area:

$$F(t)_{\text{step}} = \int_0^{r_o} (P - P_o)\, 2\pi r \cdot dr \qquad (10)$$

By using the normalized expression, equation (10) may be written by:

$$F(t)_{STEP} = 4\pi P_o r_o^2 \underline{P}_s \sum_{n=1}^{\infty} \frac{e^{-\frac{\alpha_n^2}{a}\textcircled{H}}}{\alpha_n J_1(\alpha_n)} \int_0^1 R J_o(\alpha_n R)\, dR$$

$$= 4\pi P_o r_o^2 \underline{P}_s \sum_{n=1}^{\infty} \frac{1}{\alpha_n^2} \cdot e^{-\frac{\alpha_n^2}{a}\textcircled{H}} \qquad (11)$$

where ∂_n is defined by $J_o(\alpha_n) = 0$

By operating Laplace transformation to the force function with respect to time, equation (11) can be transformed into:

$$\mathcal{L}\left\{F(t)_{STEP}\right\} = 4\pi P_o r_o^2 \underline{P}_s \sum_{n=1}^{\infty} \frac{1}{\alpha_n^2} \frac{1}{\left(s + \frac{\alpha_n^2 w}{a}\right)} \qquad (12)$$

Since the motion of the surfaces has been assumed to be a step function, the general force function with general type of input function H(t) can be represented in the form of Laplace transformation by:

$$F(s) = 4\pi P_o r_o^2 \sum_{n=1}^{\infty} \frac{1}{\alpha_n^2} \frac{1}{\left(s + \frac{\alpha_n^2 w}{a}\right)} sH(s)$$

or

$$F(s) = \frac{48\pi\mu r_o^4}{h_o^2} \sum_{n=1}^{\infty} \frac{1}{\alpha_n^4 \left(\frac{12\mu r_o^2}{\alpha_n^2 h_o^2 P_o} s + 1\right)} sH(s) \qquad (13)$$

$$J_o(\partial_n) = o$$

If the frequency of the perturbation motion is sufficiently small in comparison with cut-off frequency W_o which is defined by:

$$w_o = \frac{\partial_n^2 h_o^2 P_o}{12\mu r_o^2} \qquad (14)$$

equation (13) can be written by:

$$F(s) = \frac{48\pi\mu r_o^4}{h_o^2} \sum_{n=1}^{\infty} \frac{1}{\alpha_n^4} \cdot sH(s)$$

if $w \ll w_o$ (15)

Annular Boundary

Similar argument will give solution to equation (7) with annular boundary where the boundary conditions and initial condition are respectively:

$\underline{P}(1, \Theta) = 0$

$\underline{P}(K, \Theta) = 0$ $\qquad r_i$: inner radius

$K = r_i/r_o$ $\qquad r_o$: outer radius

$\underline{P}(R,0) = \underline{P}_s$ for a step change of H(t)

By employing the method of separation of variable, the solution of equation (7) can be expressed as follows:

$$\underline{P} = \sum_{n=1}^{\infty} \left\{ C_{1n} J_0(\partial_n R) + C_{2n} Y_0(\partial_n R) \right\} \cdot \exp.\left(-\frac{\partial_n^2}{a}\Theta\right)$$

The boundary conditions and the initial condition give the coefficients C_{1n}, and C_{2n}, and also the eigenfunction of ∂_n:

$$\underline{P} = \sum_{n=1}^{\infty} C_n \left\{ J_0(\partial_n R) - \frac{J_0(\partial_n)}{Y_0(\partial_n)} Y_0(\partial_n R) \right\} \exp.\left(-\frac{\partial_n^2}{a}\Theta\right)$$

$$C_n = \frac{\underline{P}_s \int_K^1 \left\{ J_0(\partial_n R) - \frac{J_0(\partial_n)}{Y_0(\partial_n)} Y_0(\partial_n R) \right\} R\,dR}{\int_K^1 \left\{ J_0(\partial_n R) - \frac{J_0(\partial_n)}{Y_0(\partial_n)} Y_0(\partial_n R) \right\}^2 R\,dR} \qquad (16)$$

where $J_0(\partial_n) Y_0(K\partial_n) - J_0(K\partial_n) Y_0(\partial_n) = 0$

On basis of the similar discussion to that in case of circular boundary the force function for a general input h(t) can be obtained which is expressed in Laplace transforms presentation:

$$F(s) = \frac{48\pi r_o^4 \mu}{h_o^2} \sum_{n=1}^{\infty} \frac{1}{\partial_n^4} G(\partial_n) \frac{1}{\left(\frac{12\mu r_o^2}{h_o^2 P_o \partial_n^2} S + 1\right)} \cdot SH(S) \qquad (17)$$

∂_n is defined by:

$J_0(\partial_n) Y_0(K\partial_n) = J_0(K\partial_n) Y_0(\partial_n)$, and

$G(\partial_n)$ is defined by $G(\partial_n) = \dfrac{g_1(\partial_n)}{g_2(\partial_n)}$

$$g_1(\alpha_n) = \left[\left\{ J_1(\alpha_n) - K J_1(K\alpha_n) \right\} - \frac{J_0(\alpha_n)}{Y_0(\alpha_n)} \left\{ Y_1(\alpha_n) - K Y_1(K\alpha_n) \right\} \right]^2$$

$$g_2(\alpha_n) = \left\{ J_0^2(\alpha_n) + J_1^2(\alpha_n) \right\} - K^2 \left\{ J_0^2(K\alpha_n) + J_1^2(K\alpha_n) \right\}$$
$$+ \frac{J_0^2(\alpha_n)}{Y_0^2(\alpha_n)} \left[\left\{ Y_0^2(\alpha_n) + Y_1^2(\alpha_n) \right\} - K^2 \left\{ Y_0^2(K\alpha_n) + Y_1^2(K\alpha_n) \right\} \right]$$
$$- \frac{2 J_0(\alpha_n)}{Y_0(\alpha_n)} \left[\left\{ J_0(\alpha_n) Y_0(\alpha_n) + J_1(\alpha_n) Y_1(\alpha_n) \right\} - K^2 \left\{ J_0(K\alpha_n) Y_0(K\alpha_n) \right.\right.$$
$$\left.\left. + J_1(K\alpha_n) Y_1(K\alpha_n) \right\} \right]$$

To find the zeros of the eigenfunction in equation (17), reference 4 and 5 may be consulted. If the frequency of the small perturbation is sufficiently low in comparison with the cut-off frequency w_o which is defined by:

$$w_o = \frac{h_o^2 P_o \alpha_n^2}{12 \mu r_o^2}$$

equation (17) becomes:

$$F(S) = \frac{48 \pi r_o^4 \mu}{h_o^2} \sum_{n=1}^{\infty} \frac{1}{\alpha_n^4} G(\alpha_n) \cdot SH(S) \qquad (18)$$

It is obviously seen in equation (15) and (18) that the force function is proportional to the time derivative of H(t), which reveals to give damping to dynamic systems when this mechanism exists in them. The further signigicance of these representations of the force function will be discussed in the following chapter of this paper.

Isothermal assumption

The calculation of the rate of the heat diffusibility of the gas film is needed to investigate the propriety of the isothermal assumption to the film gas. It will not be an appropriate approach to start from equation (1) unless the time constant is sufficiently small compared with the perturbation frequency.

The thickness of the gas film has been assumed to be thin enough for the assumption of creeping flow to hold, in other words, for Reynolds' number to be small enough to make inertia term negligible. This implies that the gas film can be considered to be an infinite plate bounded by massive material, the thermal conductivity of which is sufficiently large to keep its surface temperature constant through out the heat conduction. With these assumptions, the calculation is simplified to be the heat transfer problem of infinite plate with constant boundary temperature. The solution of this type of problem will be consulted in a number of references.

The governing equation is:

$$K \frac{\partial^2 \theta}{\partial^2 h} = \rho c \frac{\partial \theta}{\partial t}$$

where $\theta = T - T_o$

K: thermal conductivity of film gas

ρ: density of film gas

c: specific heat of film gas

T_o: surface temperature

According to reference 7, the solution of equation (19) with constant boundary temperature is given by:

$$\frac{\theta}{\theta_i} = \sum_{n=1}^{\infty} \frac{4}{(2n-1)\pi} e^{-\frac{(2n-1)^2 \pi^2}{h_o^2} a \cdot t} \sin \frac{(2n-1)\pi}{h_o} \cdot h$$

Therefore, the average temperature of the gas film will be obtained by integrating $\frac{\theta}{h_o}$ from o to h_o with respect to h, i.e.

$$\left(\frac{\theta}{\theta_i}\right)_{ave.} = \frac{1}{h_o} \sum_{n=1}^{\infty} \frac{4}{(2n-1)\pi} e^{-\frac{(2n-1)^2 \pi^2}{h_o^2} a t} \int_0^{h_o} \sin \frac{(2n-1)\pi}{h_o} \cdot h \, dh$$

$$= \frac{8}{\pi^2} \sum_{n=1}^{\infty} \frac{1}{(2n-1)^2} e^{-\frac{(2n-1)^2 \pi^2}{h_o^2} a t} \qquad (21)$$

$$a = \frac{K}{\rho c}$$

It is obvious to see that the maximum θ ave is given by setting t=o, i.e.

$$\left(\frac{\theta_{ave.}}{\theta_1}\right)_{max.} = \frac{8}{\pi^2}\sum_{n=1}^{\infty}\frac{1}{(2n-1)^2} = 1$$

Therefore, the following approximation for θ ave has maximum error 23.4% which vanishes as time goes on:

$$\frac{\theta_{ave.}}{\theta_1} \fallingdotseq \frac{8}{\pi^2}\, e^{-\frac{\pi^2 a t}{h_o^2}} \qquad (22)$$

The time constant of the average temperature of the gas film is represented by:

$$t_o = \frac{h_o^{\,2}}{\pi^2 a}$$

$$\text{or} = \frac{h_o^2 \rho c}{\pi^2 K} \qquad (23)$$

Reynolds' number

It is also needed to calculate Reynolds' number with some approximation in order to investigate the propriety of the assumption of creeping flow. If the fluid is incompressible, the velocity of the film fluid can be easily obtained from continuity law.

$$-v_r = \frac{r}{2h_o}\frac{dh}{dt}$$

v_r: velocity at radius r

Perturbation assumption gives:

$$|v_r|_{max.} = \frac{r_o \omega H_{max.}}{2}$$

where $H_{max.}$ is the amplitude of perturbation motion. The Reynolds' number of the film gas flow will be approximately given by:

$$R = \frac{\rho r_o \omega H_{max.}}{4\mu}$$

$$\text{or} = \frac{\pi \rho r_o f H_{max.}}{2\mu} \qquad (24)$$

where $\omega = 2\pi f$

The result of the numerical calculation of those equations obtained by the argument in this chapter will be tabulated in the following chapter.

Experiment

Apparatus

The experimental apparatus consists of a flapper, which is fixed at one end with a certain spring constant, and a pair of stationary cylindrical pads. One pad is placed on one side of the flapper, and the other is placed on the opposite side. There exists a thin air film between the flapper and the pad.

The flapper is a simple rectangular bar, the surfaces of which are carefully finished to be parallel and smooth. Two types of pads are used, one is a pair of solid cylinders, the other a pair of hollow cylinders. Each end surface of the pads, which forms with one side of the flapper air film circular or annular, depending upon which type of pad is used, is carefully finished to be normal to its axis and to be smooth.

The flapper is designed to oscillate so that some squeeze action may take place in the air films. Though the motion of the flapper cannot be parallel in a strict sense, the amplitude is so small and the lever length of the flapper is so large in comparison with the diameter of the pads, that the squeeze action of the flapper can approximately be considered to be a parallel motion where the rotational motion is negligible.

To measure the displacement of the flapper a variable differential transducer is used, the signal of which is fed through a rectifier and a filter into an oscilloscope to which a polaroid camera is connected to record the oscillation of the flapper. For adjusting the thickness of the air films, seam stocks of various thickness are used. A vacuum tube volt meter is connected to the variable differential transducer to investigate the adjusted thickness according to a previously calibrated curve.

The free oscillation of the flapper can be represented by the following dynamic equation:

$$I\ddot{\theta} + 2LF + K\theta = 0 \qquad (25)$$

I: moment of inertia of the flapper

L: length of the flapper measured from the fixed end to the center of the pads

K: spring constant

θ: angle between the neutral position and the instantaneous position of the flapper

F: force exerted by squeeze action

Laplace transformation of equation (25) reads:

$$\left(IS^2 + \frac{2LF(S)}{S\,\theta(S)} \cdot S + K\right)\theta(S) = 0 \qquad (26)$$

θ can be written by δh, i.e.

$$\theta = \delta h/L \; ; \quad \theta_o = h_o/L$$

$$\therefore \theta(S) = H(S) \cdot \theta_o$$

Therefore, equation (26) becomes an ordinary second order dynamic equation where the damping ratio ζ is

$$\zeta = \frac{L \cdot F(s)}{\omega_n I} \qquad (27)$$

$$\omega_n = \sqrt{K/I}$$

The force function F(S) has been discussed in the previous section of this paper that, if w_n is small enough compared with w_o which is defined by equation (14), F(S) becomes a constant which is independent of time derivatives of displacement. Substitution of equation (15) for circular boundary, and equation (18) for annular boundary into equation (27) represents the damping ratio for both cases:

$$\zeta_{cir} = \frac{48\pi\mu r_o^4 L^2}{\omega_n I h_o^3} \sum_{n=1}^{\infty} \frac{1}{\alpha_n^4} \qquad (28)$$

where $J_o(\partial_n) = 0$, and

$$\delta_{ann} = \frac{48\pi\mu r_o^4 L^2}{w_n I h_o^3} \sum_{n=1}^{\infty} \frac{1}{\alpha_n^4} G(\alpha_n) \qquad (29)$$

$$J_o(\alpha_n) Y_o(K\alpha_n) - J_o(K\alpha_n) Y_o(\alpha_n) = 0$$

$$K = r_i/r_o \quad ; \quad G(\alpha_n) = \frac{g_1(\alpha_n)}{g_2(\alpha_n)} \quad \text{by (17)}$$

It is seen in equation (28) and (29) that the damping ratios depend upon the viscosity of the film gas only. Ambient pressure does not affect the damping ratio as long as the natural frequency of the flapper w_n is small enough in comparison with the cut-off frequency w_o defined by

$$w_o = \frac{\alpha_n^2 h_o^2 P_o}{12\mu r_o^2}$$

To investigate the effect of ambient pressure p_o, a vacuum chamber evacuated by 6" steam ejector is used, which can obtain at most 0.15 ata. vacuum. Damping ratio is measured from recorded pictures listed from Figure A-1 to Figure A-76 through the calculation illustrated in Figure 1.

Results

The thickness of the air film was varied from 0.001" to 0.020". Ambient pressure also was varied from 1 ata. to 0.147 ata. for each thickness. Two pairs of pads, circular and annular, were used under these conditions. The recorded pictures were shown from Figure A-1 to Figure A-76 in Appendix section of this paper. The observed damping ratios and those obtained by calculation based on equation (28) and (29) were tabulated in Table A-2, and A-3 together with cut-off frequency w_o and also with $1/t_o$ which

gave the cut-off frequency where isothermal assumption breaks down. For a small perturbation method, perturbation percentage was also tabulated as Hmax in Table A-2 and Table A-3. When the chamber was being evacuated down to its lowest pressure, sucking vibration was picked up by the flapper, which was superimposed to the oscillation of the flapper itself.

Figure 2 shows the measured damping ratio under various conditions with circular pads, where the agreement between theoretically predicted values and those obtained by experiment was considerably good. Some deviation of results from the predicted line was observed, particularly in the range where the thickness was greater than 0.010". The effect of ambient pressure on damping ratio was shown in Figure 3, where the results indicated its independency of damping ratio as the theoretical analysis had predicted. The pressure 0.147 ata. was not sufficiently low to reach the critical pressure where the cut-off frequency w_o becomes comparable with the natural frequency of the flapper. This critical pressure was plotted in Figure 4 with respect to various thickness. Figure 4 indicates that vacuum of order of 10^{-4} 10^{-3} ata. was required to investigate the breakaway point with the thickness of 0.001".

In Figure 5, the results of annular boundary were plotted, where the agreement between theoretical analysis and experiment appeared considerably good.

Figure 6 shows the ambient pressure independency of damping ratio. Figure 7 indicates that in order to measure the effect of ambient pressure on damping ratio, vacuum of 10^{-4} ata. should be applied. The constants used for theoretical calculation were tabulated in Table A-1.

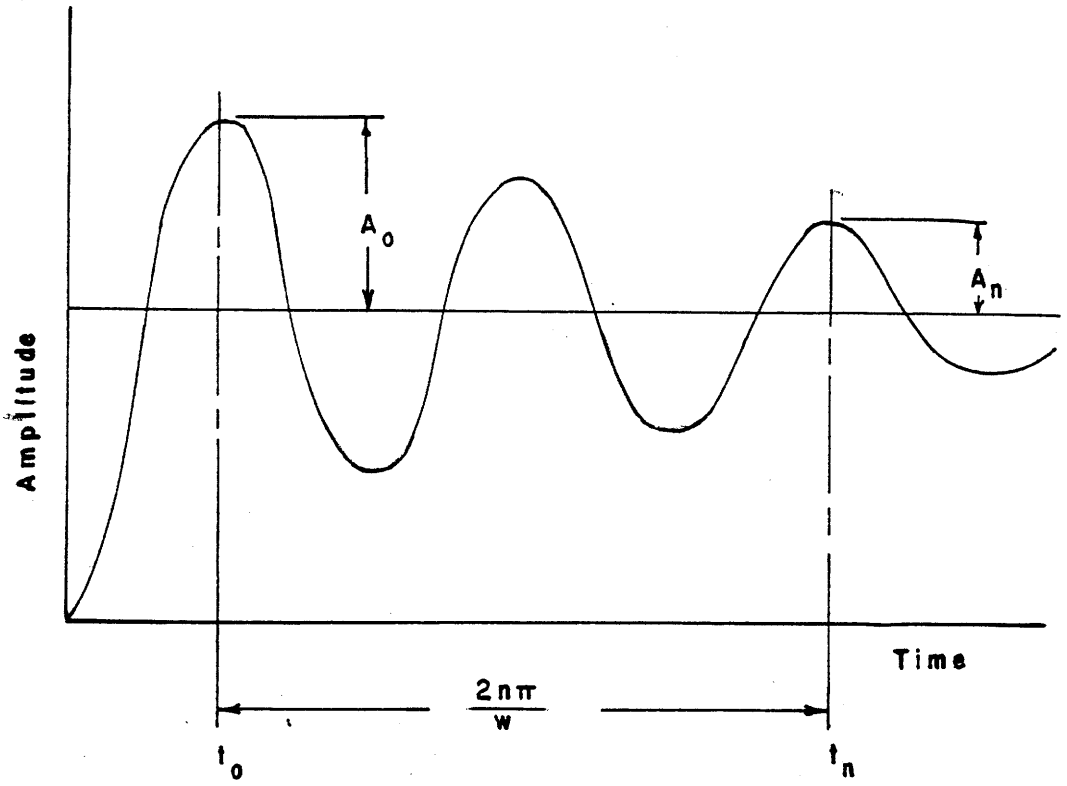

Fig·1·

$$A_0 = \alpha e^{-\zeta w_n t_0}$$

$$A_n = \alpha e^{-\zeta w_n t_n}$$

$$t_n - t_0 = \frac{2n\pi\zeta}{w_n\sqrt{1-\zeta^2}}$$

$$\ln A_0/A_n = \frac{2n\pi\zeta}{\sqrt{1-\zeta^2}}$$

$$\zeta = \frac{\ln A_0/A_n}{2n\pi}$$

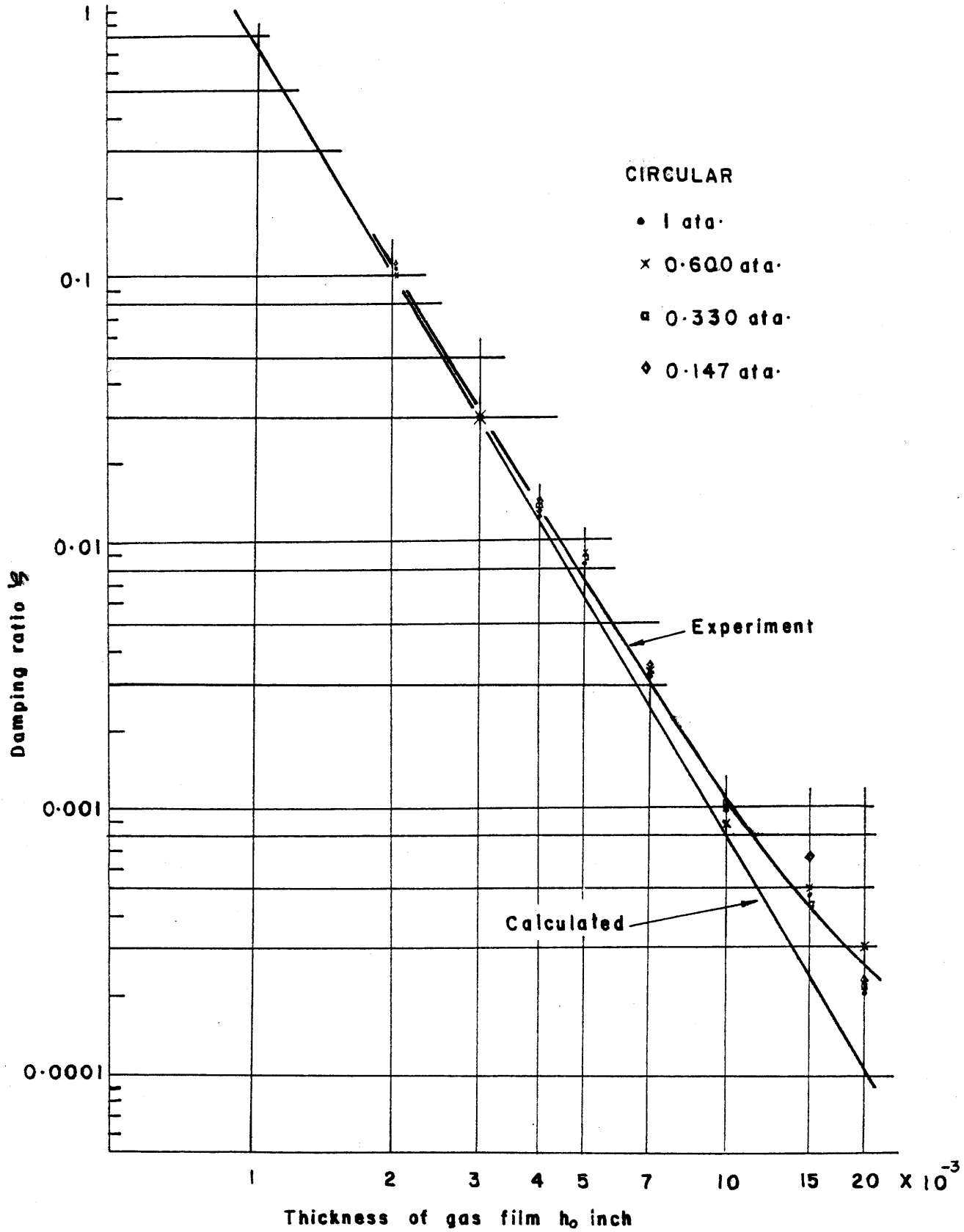
CIRCULAR
• 1 ata·
× 0·600 ata·
▫ 0·330 ata·
◆ 0·147 ata·
Experiment
Calculated
Damping ratio
1
0·1
0·01
0·001
0·0001
1
2
3
4
5
7
10
15
20
X 10⁻³
Thickness of gas film h₀ inch

Fig·2·

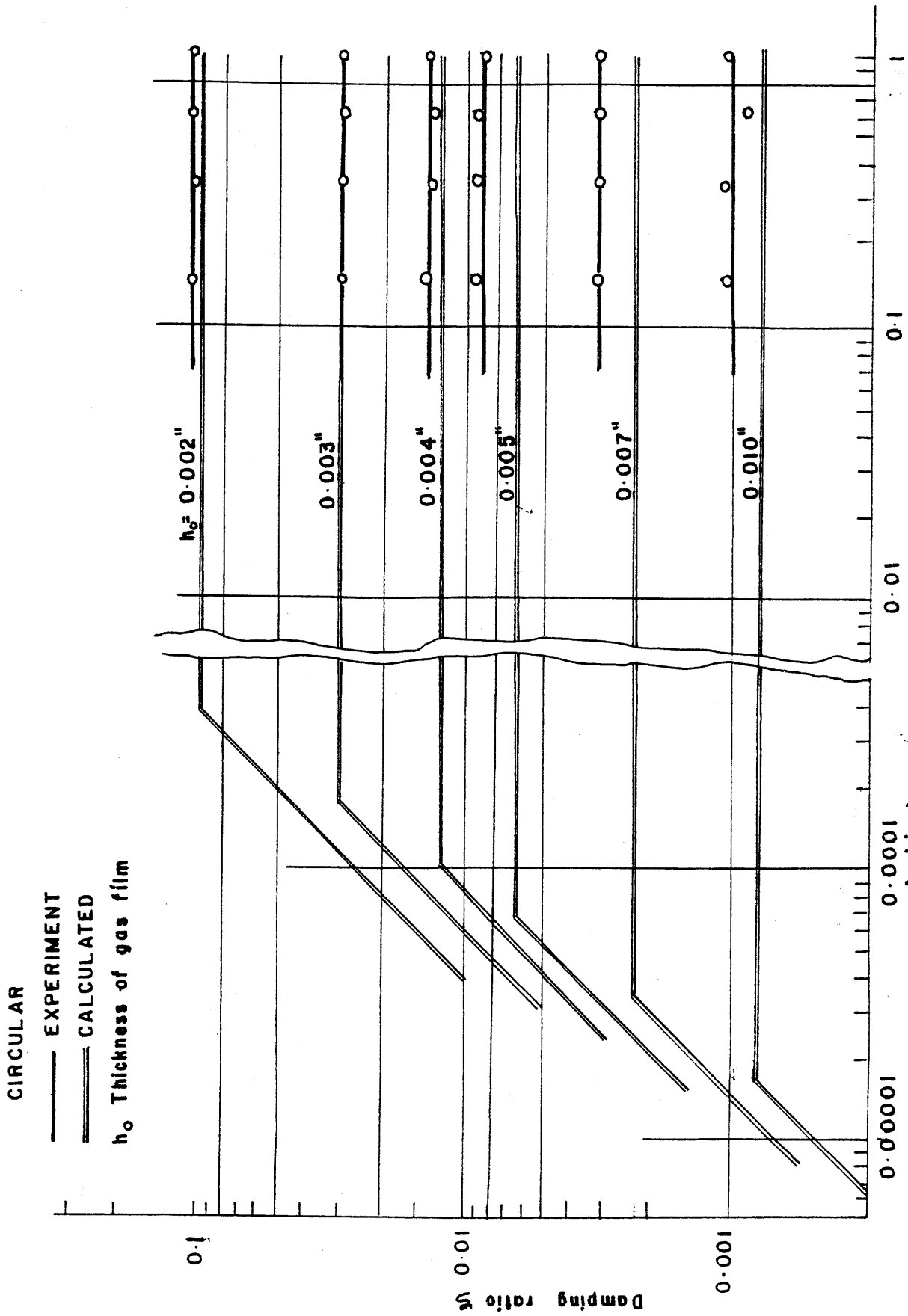

EFFECT OF AMBIENT PRESSURE ON DAMPING RATIO.

Fig·3.

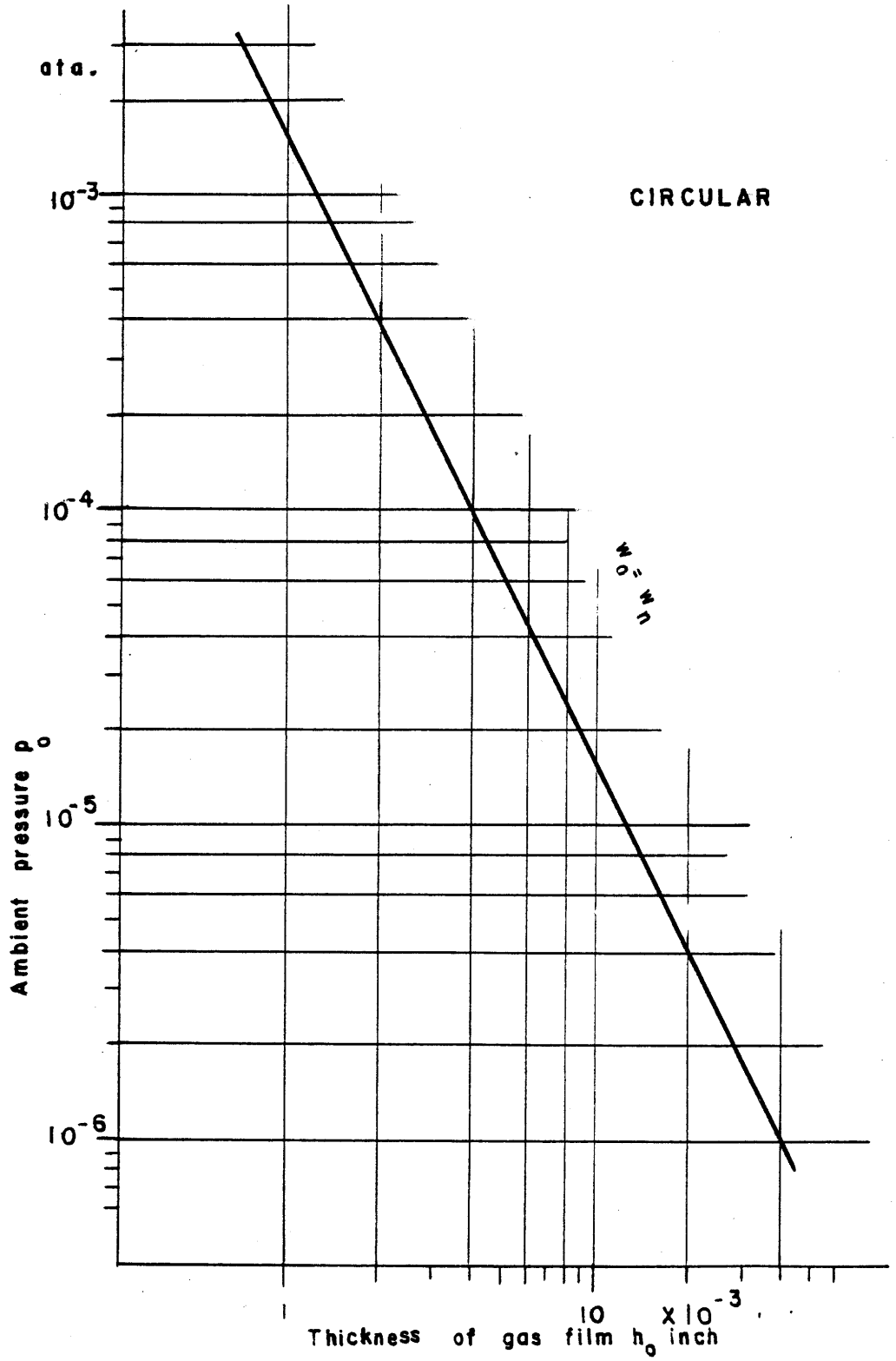

Fig. 4. CUT-OFF FREQUENCY LINE

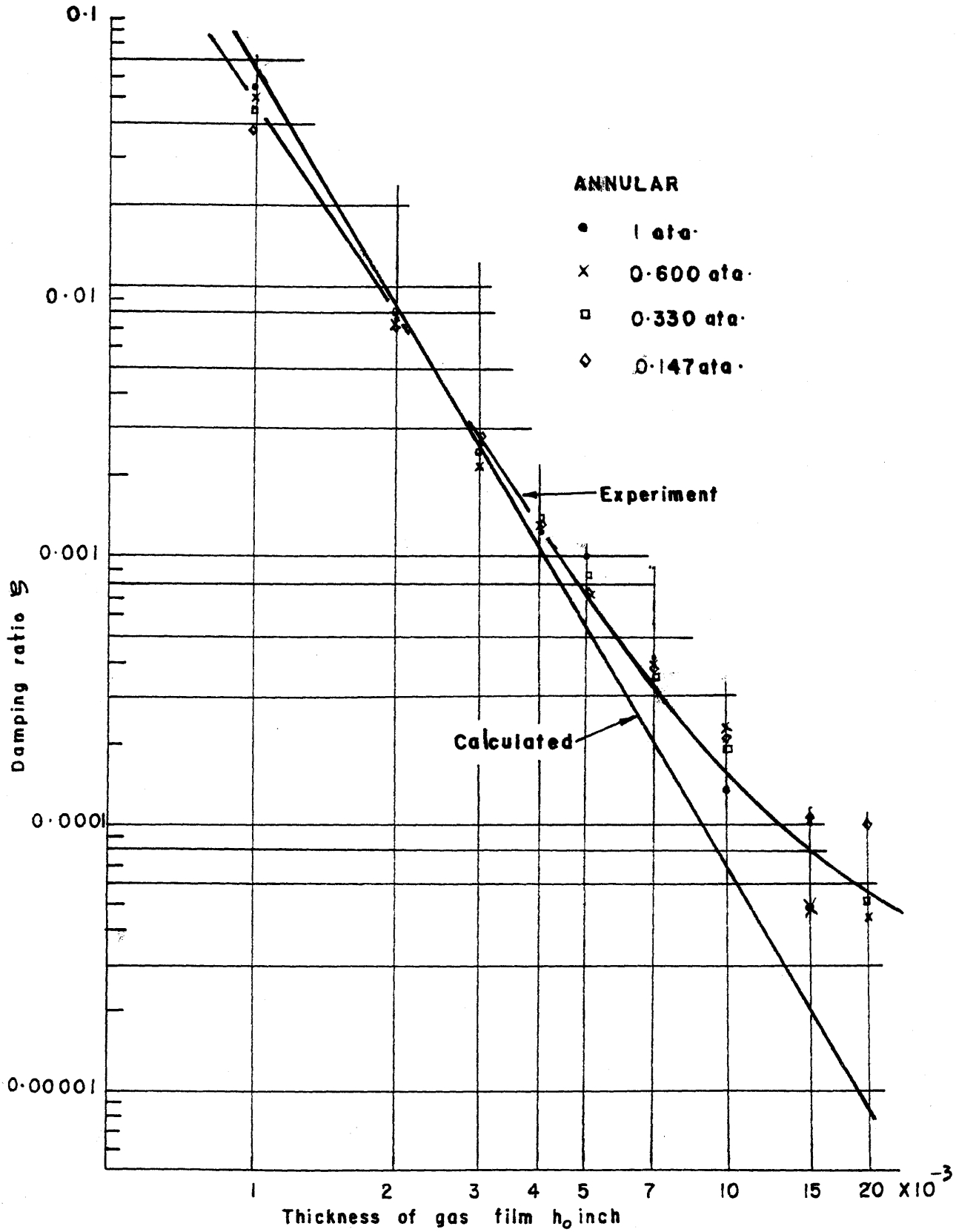
0·1
0·01
0·001
0·0001
0·00001
Damping ratio δ
ANNULAR
• 1 ata·
× 0·600 ata·
□ 0·330 ata·
◇ 0·147 ata·
Experiment
Calculated
1
2
3
4
5
7
10
15
20
X10⁻³
Thickness of gas film h₀ inch

Fig·5·

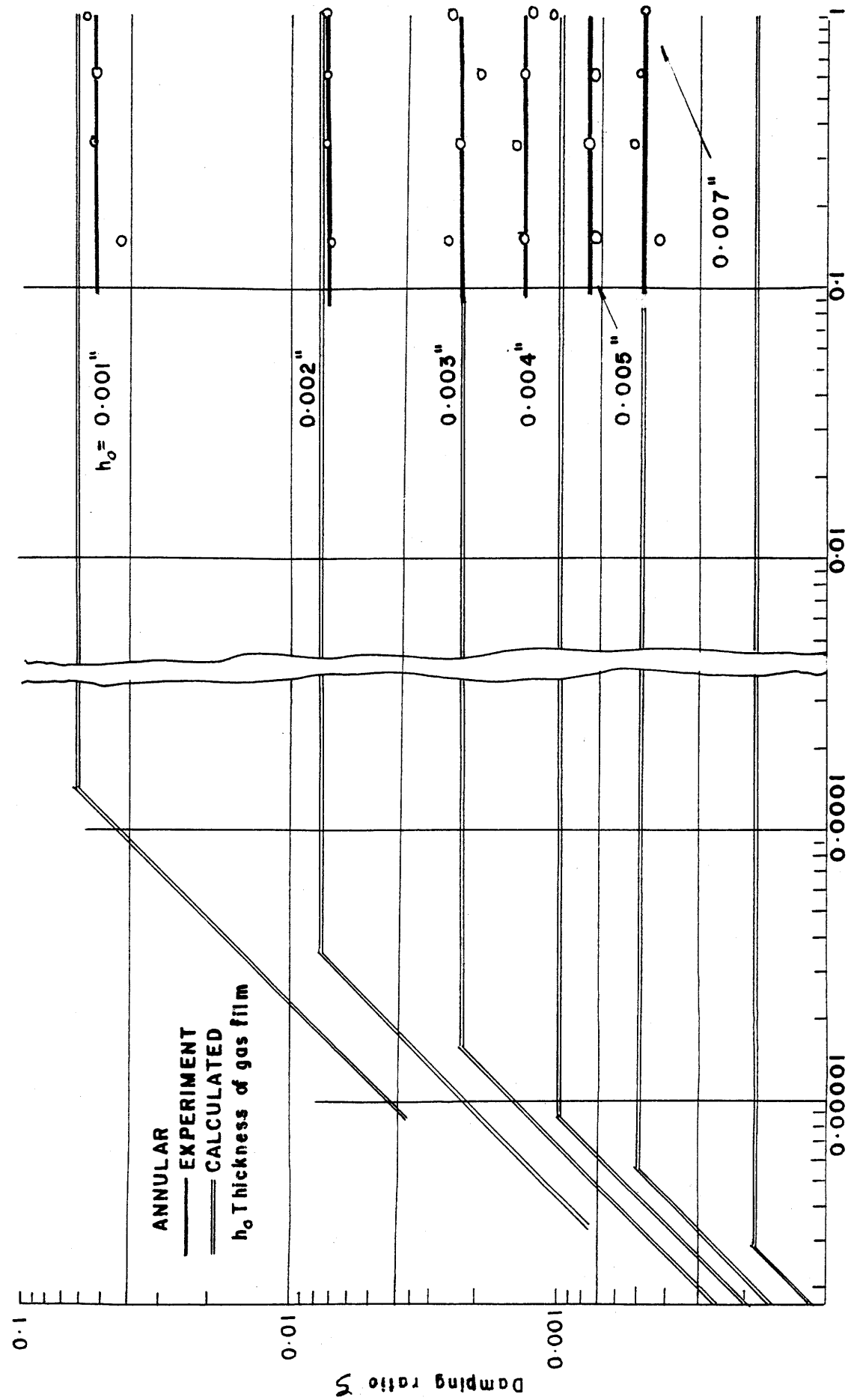

EFFECT OF AMBIENT PRESSURE ON DAMPING RATIO

Fig·6·

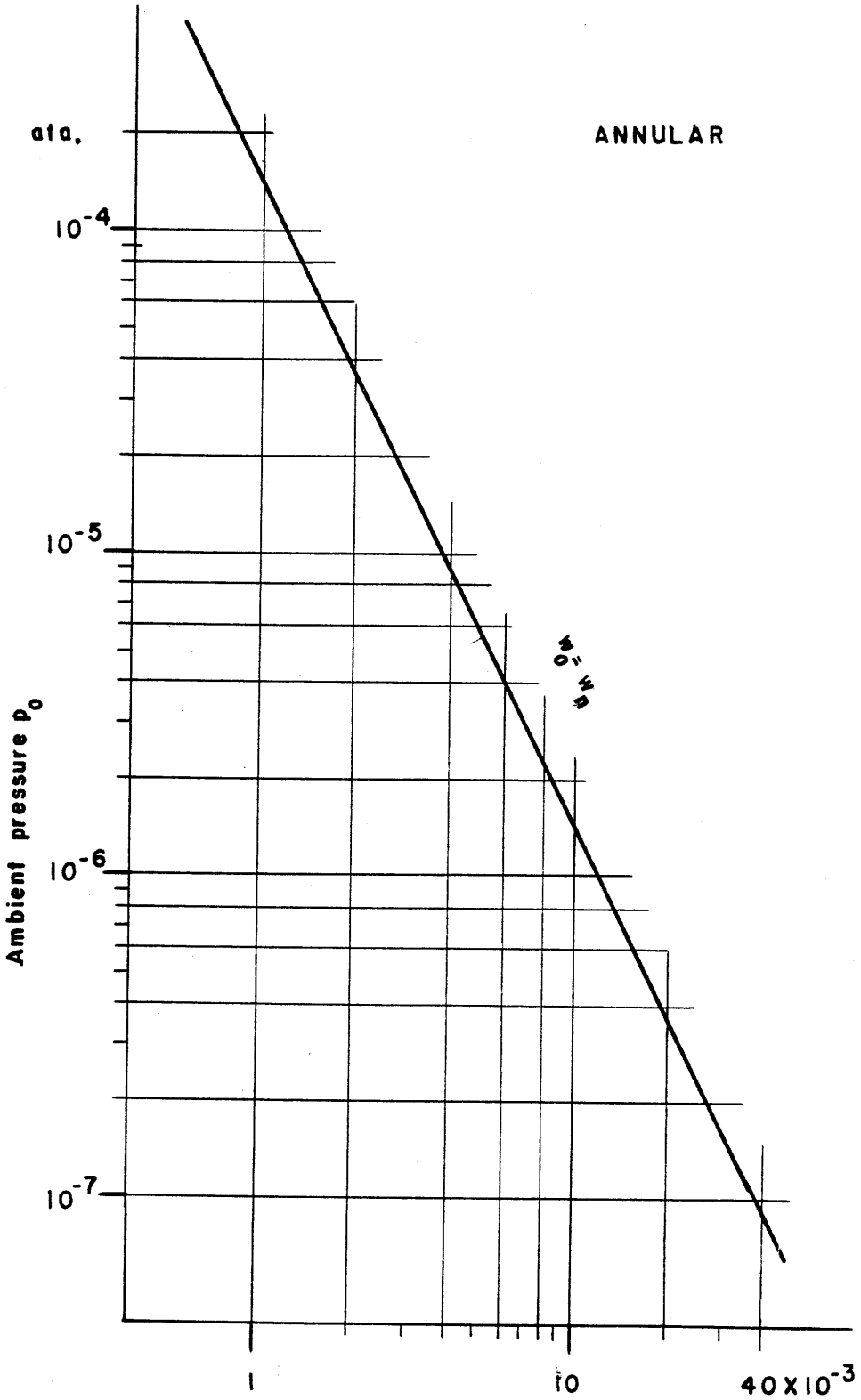

Fig·7· CUT-OFF FREQUENCY LINE

Discussion

The assumptions of the isothermal change and the creeping flow of the film air, and also the approach of the small perturbation motion of the moving surface should be reviewed here again on the basis of the numerical calculations tabulated in the Appendix section of this paper. The time constants of the heat conduction of the air films at various thickness, which are listed in Table A-2 and Table A-3 as reciprocal $1/t_o$ (sec^{-1}), appear sufficiently small in all cases as far as this experiment was concerned; for instance, the time constant of the circular film of 0.020" thickness was calculated to be $1.26X10^{-3}$ sec., under atmospheric pressure, while the natural frequency of the flapper was 47.8 c.p.s. The isothermal assumption might have been preserved in this experiment as long as the thickness of air film was less than 0.046" under atmospheric pressure.

Regarding the effect of ambient pressure on damping ratio, as the theoretical analysis predicted that the ambient pressure p_o will remain independent of damping effect as long as it is less than the critical pressure where the cut-off frequency w_o defined by equation (14) becomes close to the natural frequency of the flapper w_n, the results of this experiment showed its independency of damping effect in the range from atmospheric pressure down to 0.147 ata. As was shown in Figure 2 and Figure 5, some deviation of the results of the experiment from those predicted by the analysis was observed in both circular and annular cases, particularly at the thickness over 0.010". The damping ratio itself seemed to be too small to distinguish it from that due to the free oscillation of the flapper in absence of air films. The net damping effect due to the squeeze action is to be calculated by subtracting the observed damping ratio by that due to the free oscillation. Therefore, it may be possible that a large amount of error remained in the net subtracted damping ratio.

As to the creeping flow assumption, attention should be paid to Reynolds' number. As a rough approximation, the assumption of incompressibility was employed to calculate the Reynolds' number

of the flow in the air film, which was represented in the form of equation (24) in the previous section of this paper. The numerical calculation of the Reynolds' number at the thickness of air films was 0.020" with 10 per cent of perturbation was .130 which indicated that the assumption of creeping flow was preserved in safety.

Since the small perturbation motion was assumed to linearize the relation between the squeeze action and the pressure distribution of gas films, the percentage of the perturbation was labeled to each result of this experiment in Table A-2 and Table A-3, which was small enough particularly when the thickness of the air films was over 0.010" where the deviation became remarkable. Therefore, this deviation still cannot be explained from this point of view.

It may be possible to imagine that some particular flow pattern of the air exists about the oscillating flapper without any pads. Once the pads are placed with a considerably large thickness of the air film where the effect of squeeze action becomes no longer appreciable, quite a different flow pattern from that induced by the free oscillation in absence of the pads will be formed, which may give a certain amount of damping effect independently of squeeze action. The consideration of this flow pattern may possibly explain the observed deviation.

Conclusion

In general, the agreement between the theory and the experiment was acceptable. For further investigation of the theoretical analysis discussed in this paper, the use of a small thermal conductivity material for the pads may reveal the information on difference in damping effect between an isothermal change and an adiabatic process. A higher vacuum which could not be attained in this experiment may be helpful to visualize the pressure effect on squeeze action damping in the vicinity where the ambient pressure gives the cut-off frequency w_o equal to the natural frequency of the flapper w_n.

Since the time assigned to this study was limited, the theoretical approach discussed in this paper has remained to be an approximation for the study of squeeze action damping of gas films, and the related experiment also has left something to be studied in more detail.

In conclusion, a more detailed study will be expected to pursue the dynamic behavior of squeeze gas films in the future.

APPENDIX

Table of Constants

notation		constant	unit
$\sqrt{K/I} = \omega_n$	:	natural frequency of flapper	47.8 c/s
I	:	moment of inertia of flapper	10,300 gr-cm^2
k	:	thermal conductivity of air	6.05×10^{-5} cal/cm-sec.$^\circ$K
μ	:	viscosity of air	1.799×10^{-4} gr/cm-sec
c	:	specific heat of air	0.2500 cal/gr$^\circ$K
r_i	:	inner radius of annular pad	0.484 cm
r_o	:	outer radius of pad	0.780 cm
∂_n	:	zeros of J_o	

n	1	2	3	4	
∂_n	2.4048	5.5201	8.6537	11.7915	

∂_n : $J_o(\alpha_n)Y_o(k\alpha_n) - J_o(k\alpha_n)Y_o(\alpha_n) = 0$; $k = r_i/r_o$

n	1	2			
∂_n	8.240	18.434			

Table A-1

Results of Experiment and Calculation

notations:

h_o: Thickness of air film

p_o: ambient pressure

ζ': observed damping ratio

ζ: net damping ratio $(\zeta' - \zeta'_{h_o=\infty})$

ζ_{th}: theoretically predicted damping ratio

$H_{max.}$: perturbation percentage

w_o: cut-off frequency calculated by equation (14)

t_o: time constant of heat conduction of air film calculated by equation (24)

h_o in.	P_o ata.	δ'	δ	δ_{th}	H_{max} %	W_o $\times 10^3$	$1/t_o$ $\times 10^3$
∞	1	0.00117					
∞	0.600	0.00117		※ No over-shoot was observed			
∞	0.330	0.00116					
∞	0.147	0.00110					
0.001	1	※		0.778		31.0	318
0.001	0.60	※		0.778		18.6	523
0.001	0.33	※		0.778		10.3	986
0.001	0.147	※		0.778		4.55	1420
0.002	1	0.105	0.64	0.0972	23	124	79.5
0.002	0.600	0.104	0.103	0.0972	23	74.5	131
0.002	0.330	0.102	0.101	0.0972	23	41.2	247
0.002	0.147	0.107	0.106	0.0972	23	18.2	355
0.003	1	0.0307	0.0295	0.0288	25	279	35.4
0.003	0.600	0.0299	0.0287	0.0288	25	167	58.5
0.003	0.330	0.0307	0.0295	0.0288	25	92.7	110
0.003	0.147	0.0303	0.0292	0.0288	25	41.0	158
0.004	1	0.0145	0.0133	0.0122	15	496	19.9
0.004	0.600	0.0144	0.0132	0.0122	15	297	33.0
0.004	0.330	0.0147	0.0135	0.0122	15	165	62.0
0.004	0.147	0.0153	0.0142	0.0122	15	72.9	89.0

h_o in.	P_o ata.	ε'	ε	ε_{th}	H_{max} %	W_o x10³	$1/t_o$ x10³
0.005	1	0.00970	0.00853	0.00623	20	775	12.7
0.005	0.600	0.1105	0.00933	0.00623	20	465	20.0
0.005	0.330	0.0103	0.00913	0.00623	20	258	39.4
0.005	0.147	0.0101	0.00900	0.00623	20	114	56.7
0.007	1	0.00440	0.00323	0.00227	18	1520	6.52
0.007	0.600	0.00448	0.00331	0.00227	18	910	10.8
0.007	0.330	0.00462	0.00346	0.00227	18	505	20.2
0.007	0.147	0.00453	0.00343	0.00227	18	223	29.1
0.010	1	0.00220	0.00103	0.000778	12.5	3100	3.18
0.010	0.600	0.00203	0.00086	0.000778	12.5	1860	5.26
0.010	0.330	0.00223	0.00107	0.000778	12.5	1030	9.87
0.010	0.147	0.00216	0.00106	0.000778	12.5	456	14.2
0.015	1	0.00164	0.00047	0.000231	10	6980	1.42
0.015	0.600	0.00167	0.00050	0.000231	10	4180	2.34
0.015	0.330	0.00157	0.00041	0.000231	10	2320	4.48
0.015	0.147	0.00179	0.00069	0.000231	10	1025	6.33
0.020	1	0.00137	0.00020	0.0000972	8	12400	0.795
0.020	0.600	0.00147	0.00030	0.0000972	8	7440	1.31
0.020	0.330	0.00137	0.00021	0.0000972	8	4120	2.47
0.020	0.147	0.00134	0.00024	0.0000972	8	1820	3.55

Table A-2 (Circular continued)

h_o in	P_o ata	ζ'	ζ	$\zeta_{th.}$	H_{max} %	W_o $\times 10^3$	$1/t_o$ $\times 10^3$
0.001	1	0.0596	0.0584	0.0636	50	340	318
0.001	0.600	0.0550	0.0538	0.0636	50	204	525
0.001	0.330	0.0540	0.0528	0.0636	50	113	987
0.001	0.147	0.0447	0.0436	0.0636	50	50	1420
0.002	1	0.00875	0.00758	0.00795	15	1360	79.5
0.002	0.600	0.00860	0.00743	0.00795	15	815	131
0.002	0.330	0.00892	0.00776	0.00795	15	452	247
0.002	0.147	0.00818	0.00708	0.00795	15	200	355
0.003	1	0.00361	0.00244	0.00236	24	3060	35.4
0.003	0.600	0.00313	0.00196	0.00236	24	1830	58.5
0.003	0.330	0.00353	0.00237	0.00236	24	1010	110
0.003	0.147	0.00366	0.00256	0.00236	24	450	158
0.004	1	0.00238	0.00121	0.000995	27	5430	19.9
0.004	0.600	0.00253	0.00136	0.000995	27	3250	33.0
0.004	0.330	0.00260	0.00144	0.000995	27	1810	62.0
0.004	0.147	0.00243	0.00133	0.000995	27	800	89.0
0.005	1	0.00220	0.00103	0.000510	25	8500	12.7
0.005	0.600	0.00189	0.00072	0.000510	25	5100	20.0
0.005	0.330	0.00202	0.00086	0.000510	25	2830	39.4
0.005	0.147	0.00183	0.00073	0.000510	25	1250	56.7

h_o in.	P_o ata.	ζ'	ζ	ζ th.	H_{max} %	W_o x10³	$1/t_o$ x10³
0.007	1	0.00166	0.00049	0.000186	21	16500	6.52
0.007	0.600	0.00166	0.00049	0.000186	21	10000	10.8
0.007	0.330	0.00168	0.00052	0.000186	21	5550	20.2
0.007	0.147	0.00152	0.00042	0.000186	21	2450	29.1
0.010	1	0.00130	0.00013	0.0000636	13	34000	3.18
0.010	0.600	0.00142	0.00025	0.0000636	13	20350	5.26
0.010	0.330	0.00137	0.00021	0.0000636	13	11300	9.87
0.010	0.147	0.00133	0.00023	0.0000636	13	5000	14.2
0.015	1	0.00122	0.00005	0.0000189	7	76400	1.42
0.015	0.600	0.00115	0.000000	0.0000189	7	45900	2.34
0.015	0.330	0.00121	0.00005	0.0000189	7	25400	4.48
0.015	0.147	0.00121	0.00011	0.0000189	7	11250	6.33
0.020	1	0.00117	0.00000	0.00000795	6	136000	0,795
0.020	0.600	0.00121	0.00004	0.00000795	6	81500	1.31
0.020	0.330	0.00121	0.00005	0.00000795	6	45200	2.47
0.020	0.147	0.00121	0.00011	0.00000795	6	20000	3.55

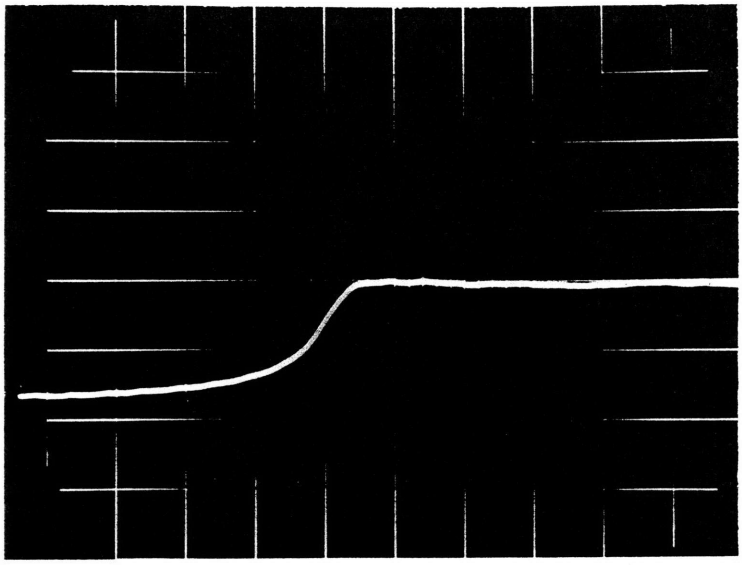

Fig. A-1

(Circular 0.001" 1 ata.)

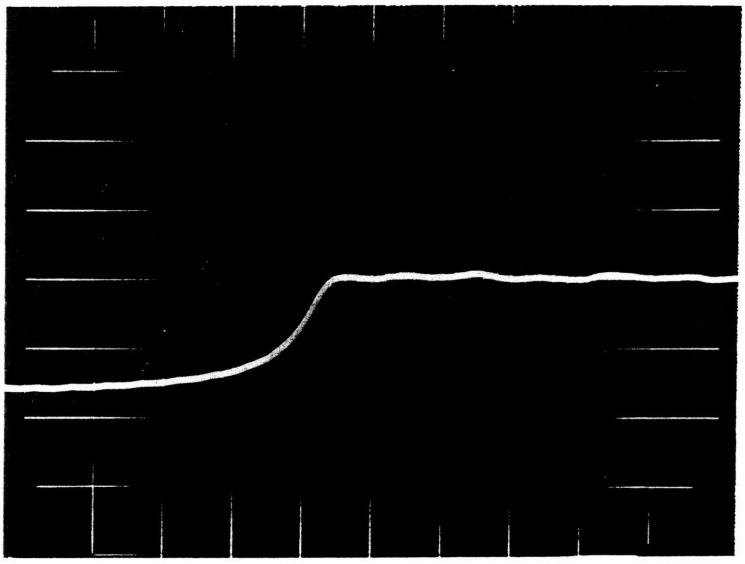

Fig. A-2

(Circular 0.001" 0.600 ata.)

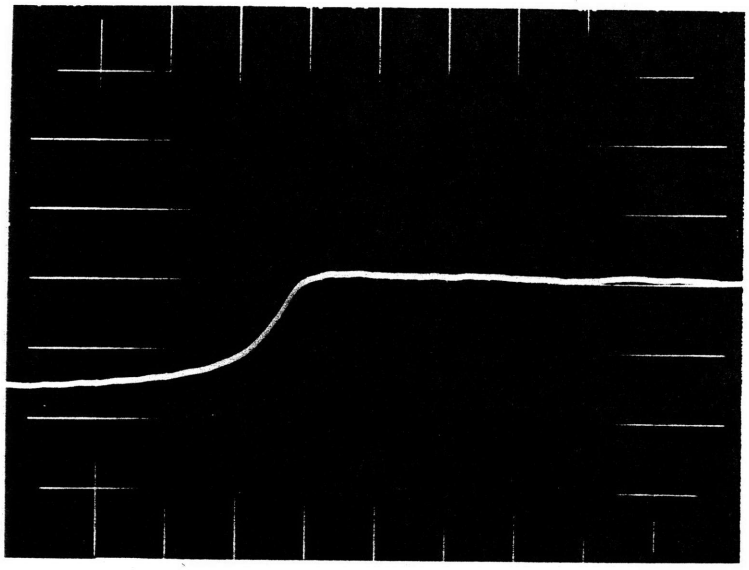

Fig. A-3

(Circular 0.001" 0.330 ata.)

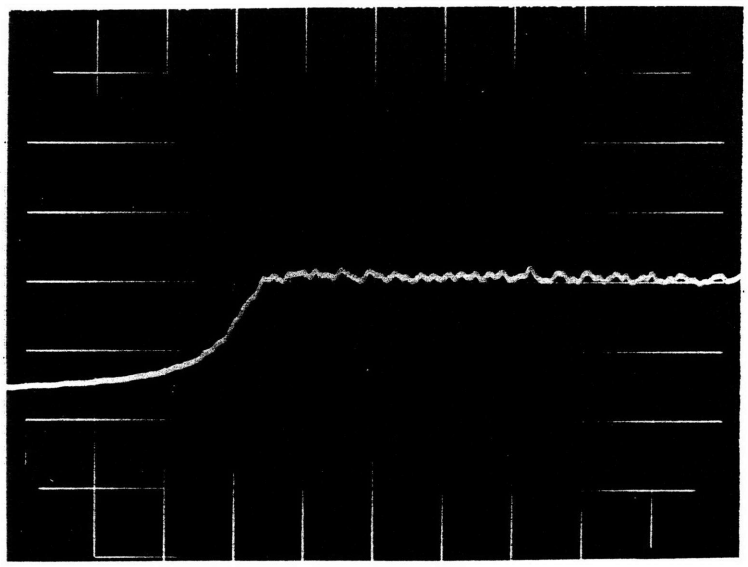

Fig. A-4

(Circular 0.001" 0.147 ata.)

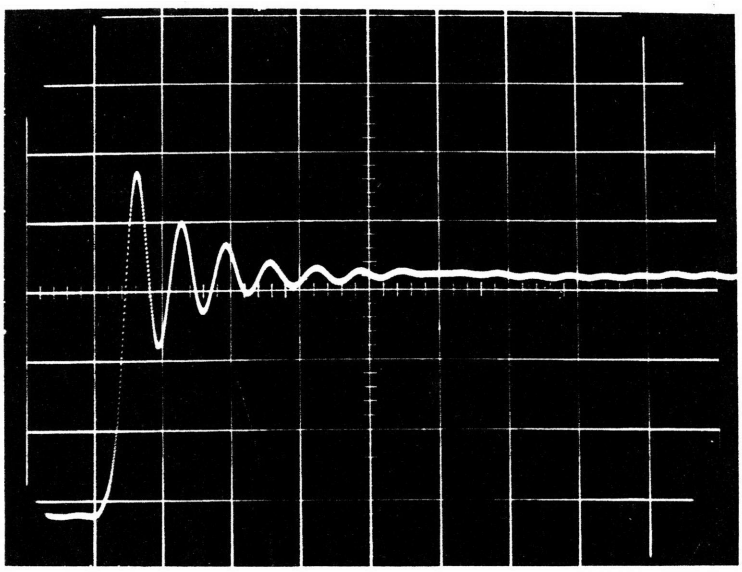

Fig. A-5

(Circular 0.002" 1 ata.)

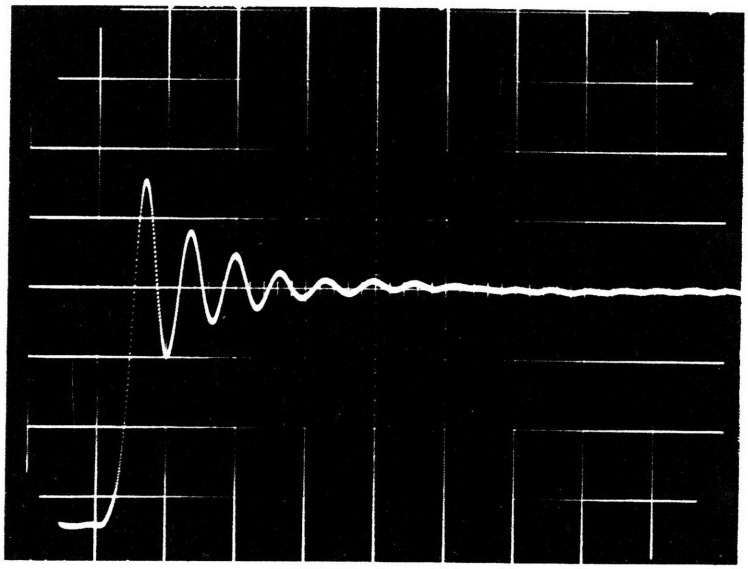

Fig. A-6

(Circular 0.002" 0.600 ata.)

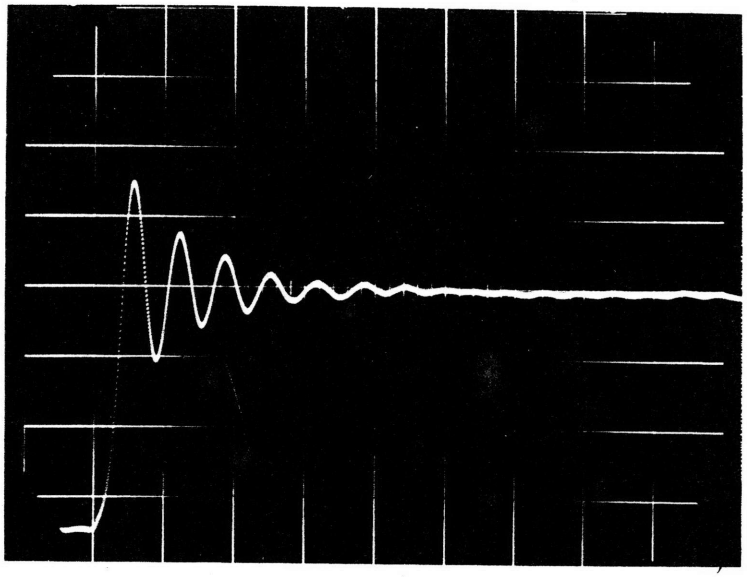

Fig. A-7

(Circular 0.002" 0.330 ata.)

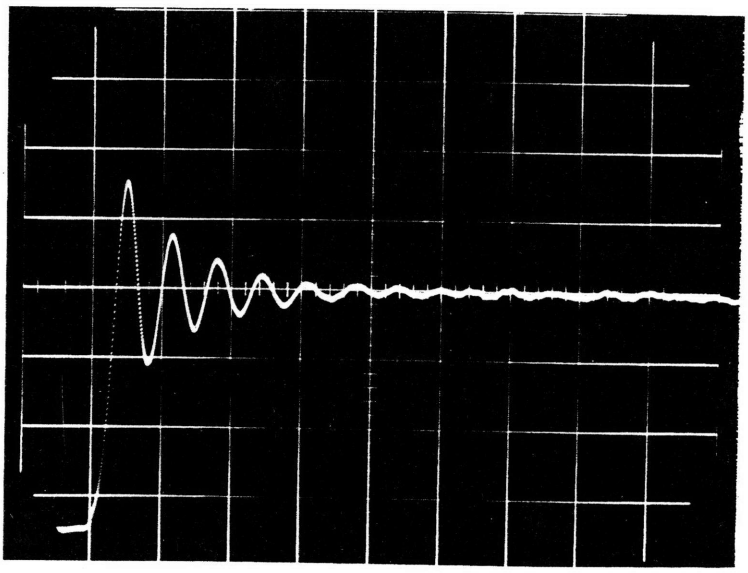

Fig. A-8

(Circular 0.002" 0.147 ata.)

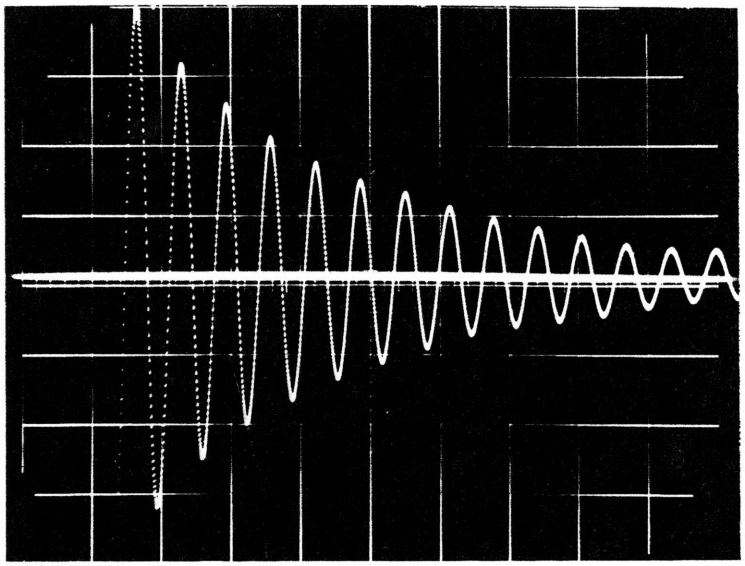

Fig. A-9

(Circular 0.003" 1 ata.)

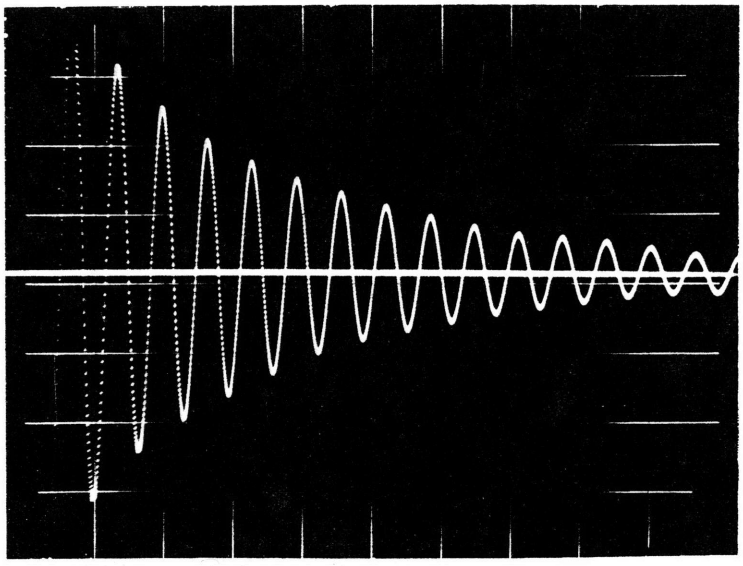

Fig. A-10

(Circular 0.003" 0.600 ata.)

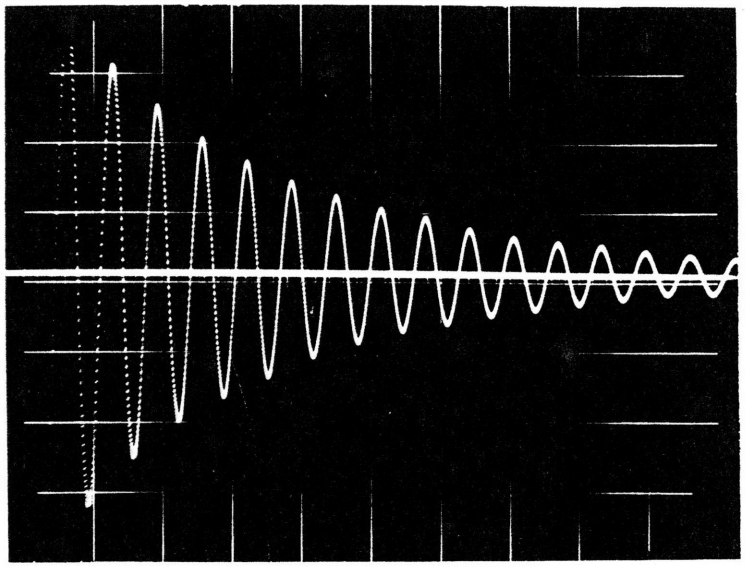

Fig. A-11

(Circular 0.003" 0.330 ata.)

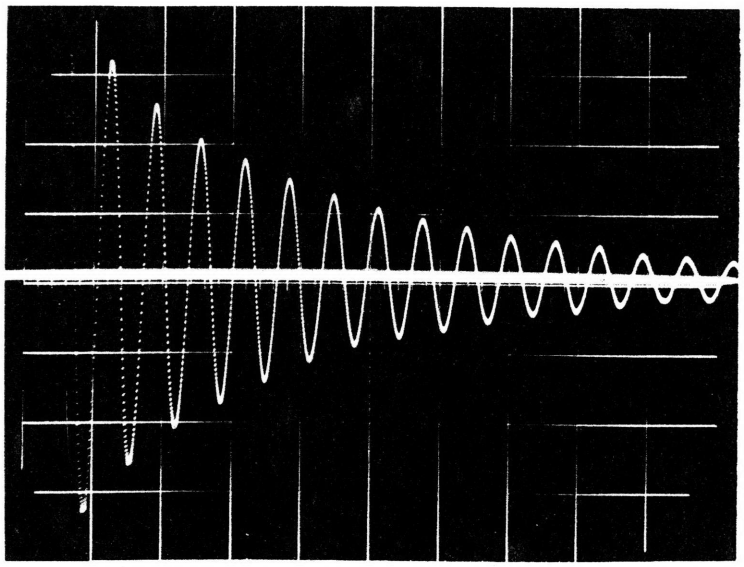

Fig. A-12

(Circular 0.003" 0.147 ata.)

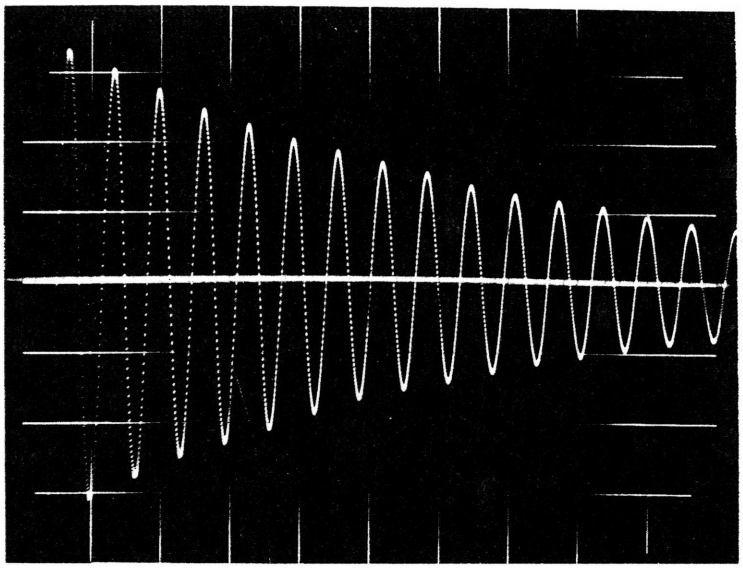

Fig. A-13

(Circular 0.004" 1 ata.)

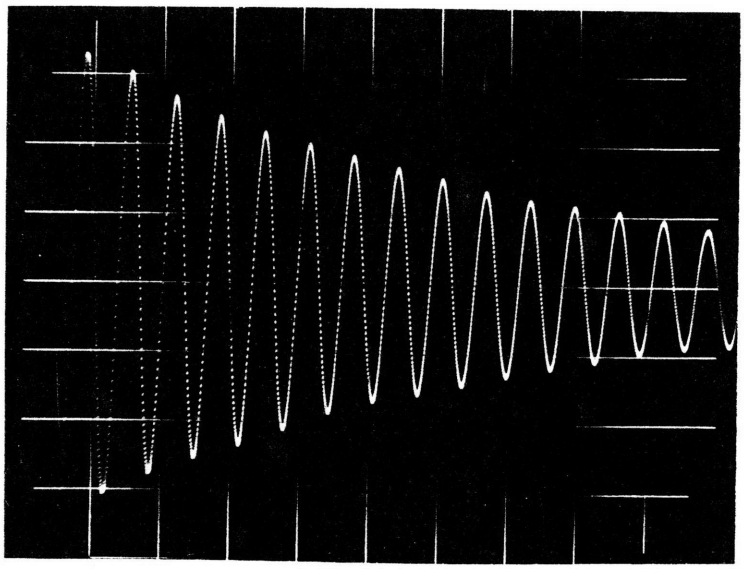

Fig. A-14

(Circular 0.004" 0.600 ata.)

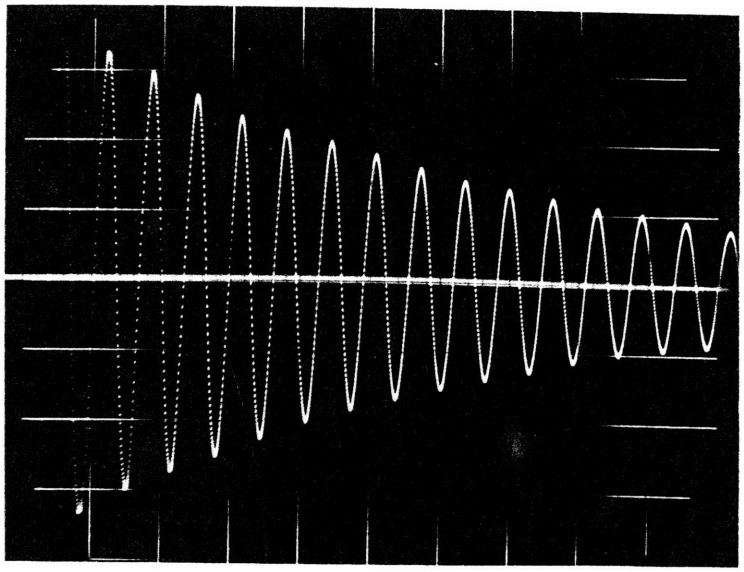

Fig. A-15

(Circular 0.004" 0.330 ata.)

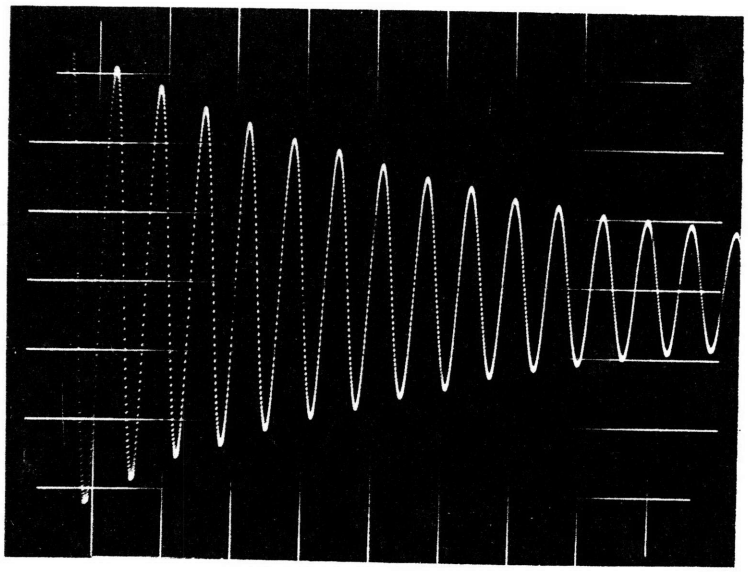

Fig. A-16

(Circular 0.004" 0.147 ata.)

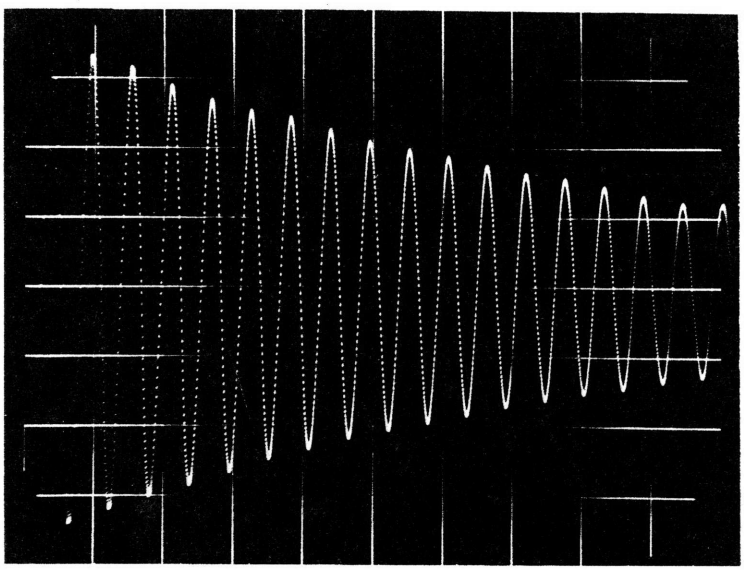

Fig. A-17

(Circular 0.005" 1 ata.)

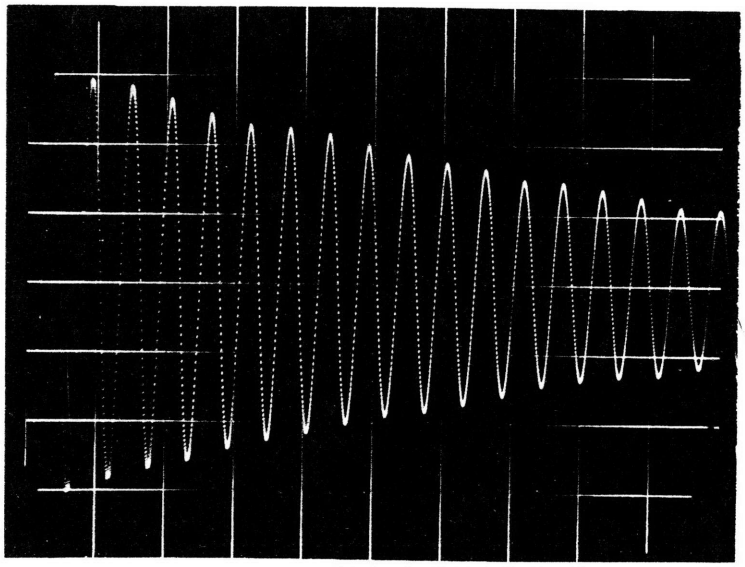

Fig. A-18

(Circular 0.005" 0.600 ata.)

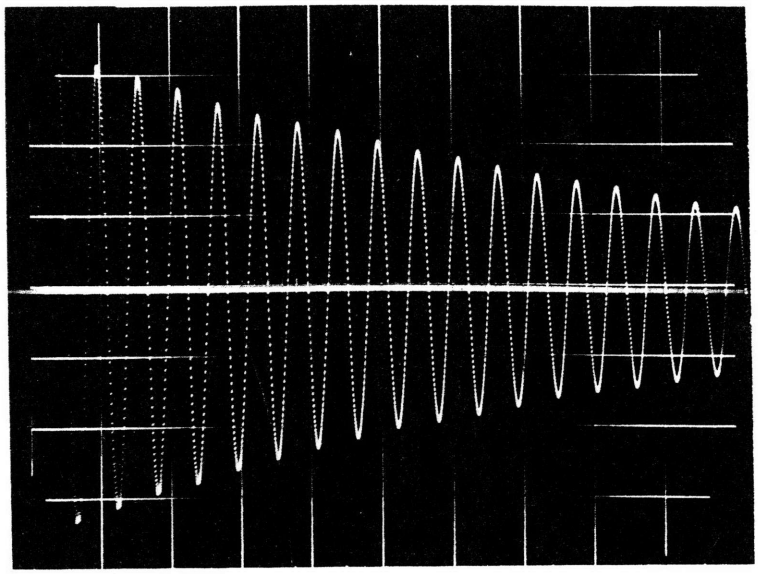

Fig. A-19

(Circular 0.005" 0.330 ata.)

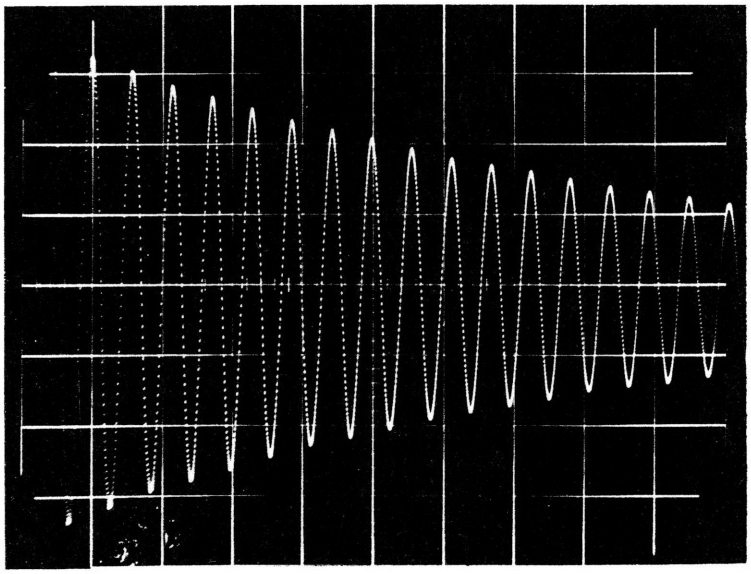

Fig. A-20

(Circular 0.005" 0.147 ata.)

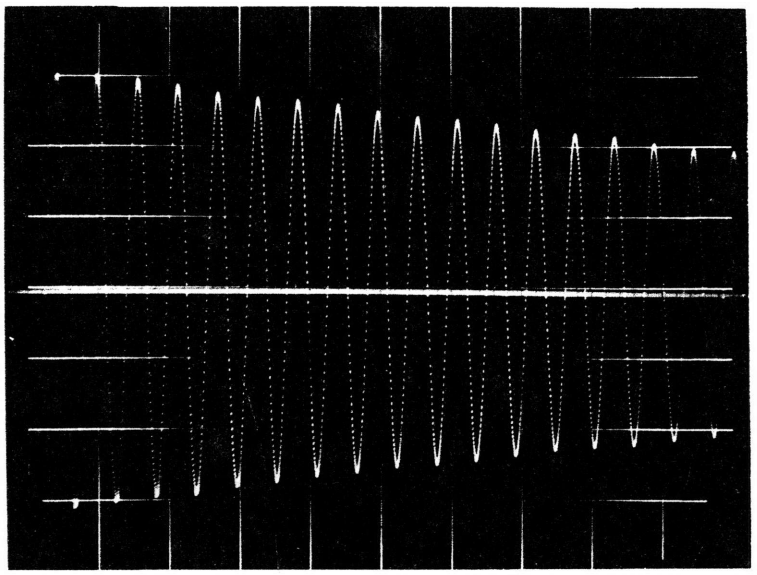

Fig. A-21

(Circular 0.007" 1 ata.)

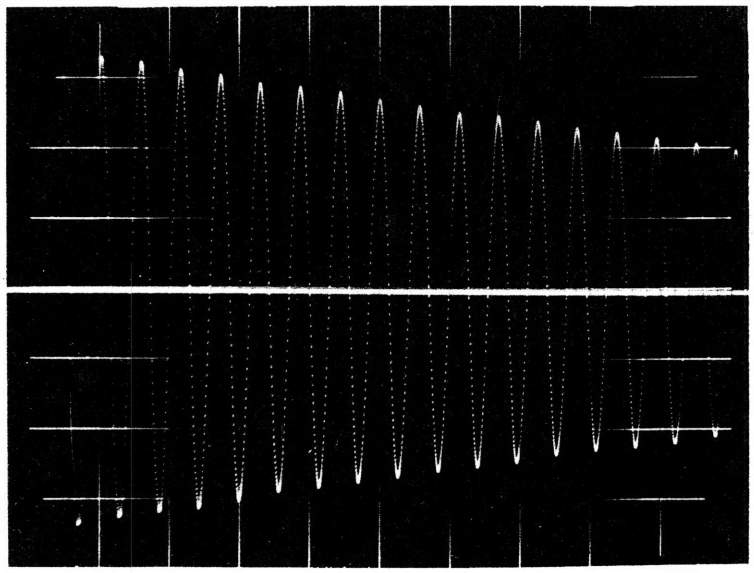

Fig.A-22

(Circular 0.007" 0.600 ata.)

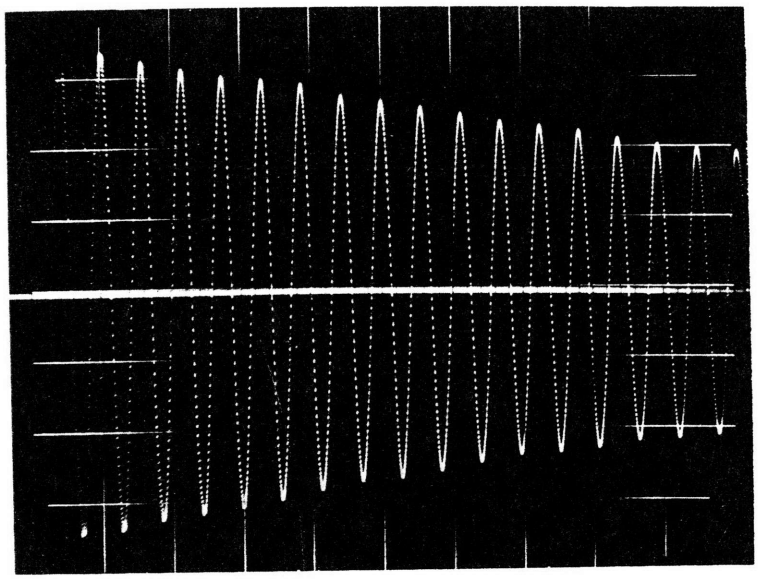

Fig. A-23

(Circular 0.007" 0.330 ata.)

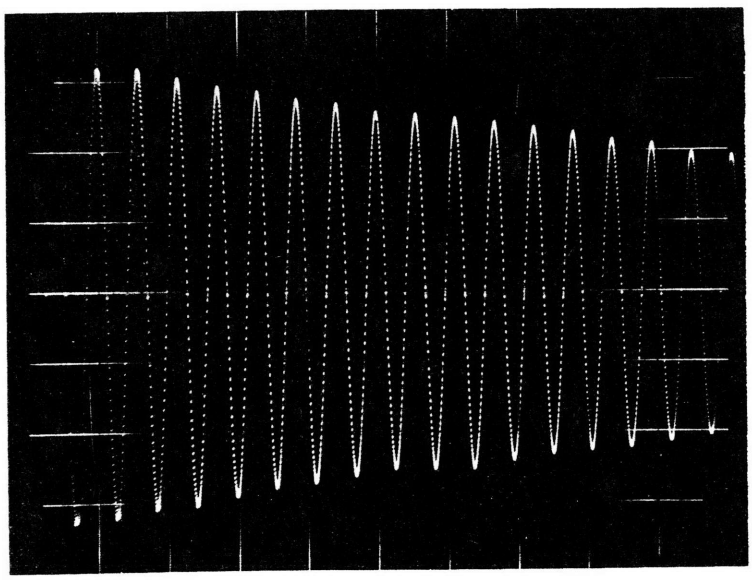

Fig. A-24

(Circular 0.007" 0.147 ata.)

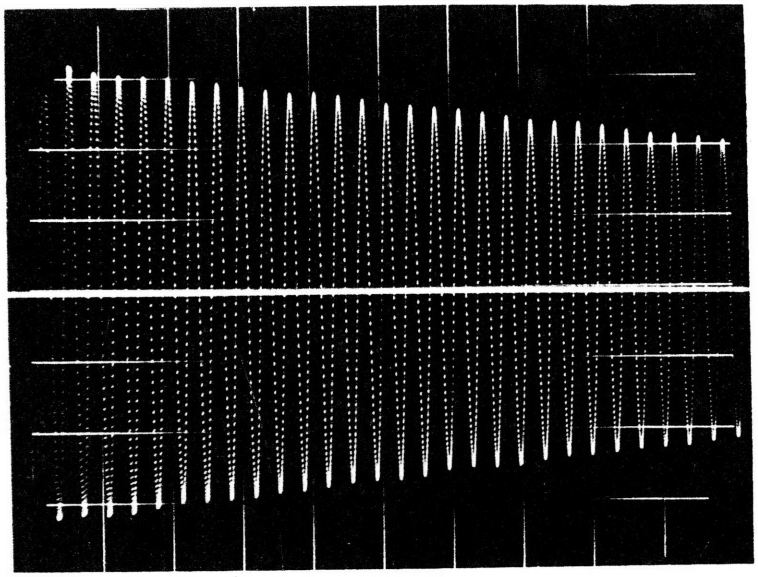

Fig. A-25

(Circular 0.010" 1 ata.)

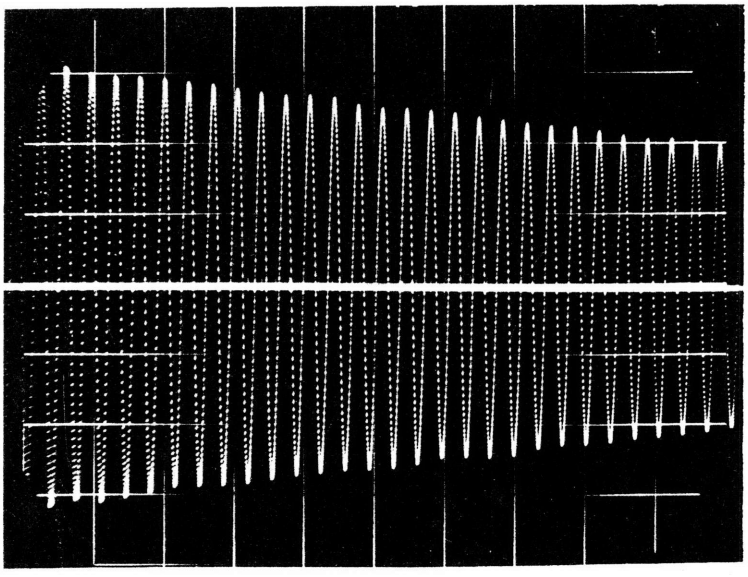

Fig. A-26

(Circular 0.010" 0.600 ata.)

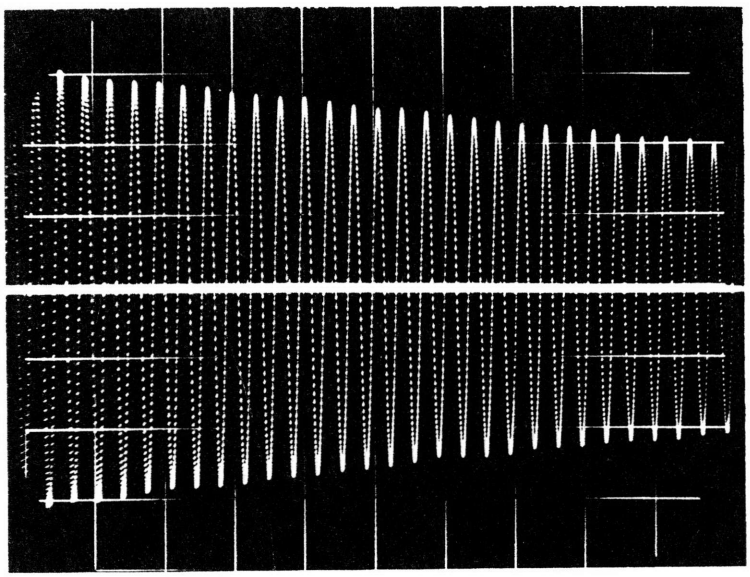

Fig. A-27

(Circular 0.010" 0.330 ata.)

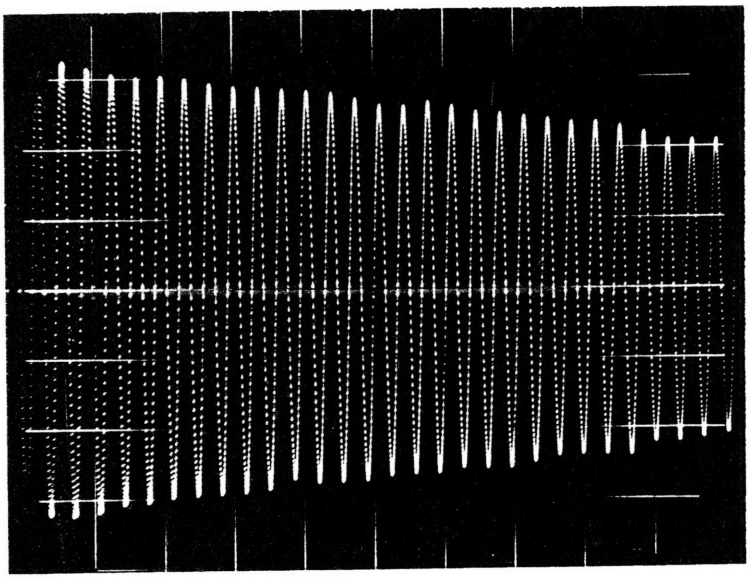

Fig. A-28

(Circular 0.010" 0.147 ata.)

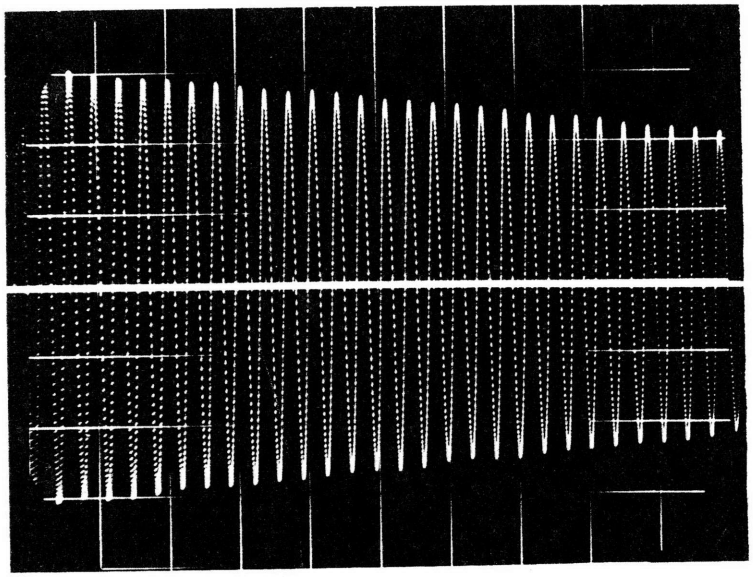

Fig. A-29

(Circular 0.015" 1 ata.)

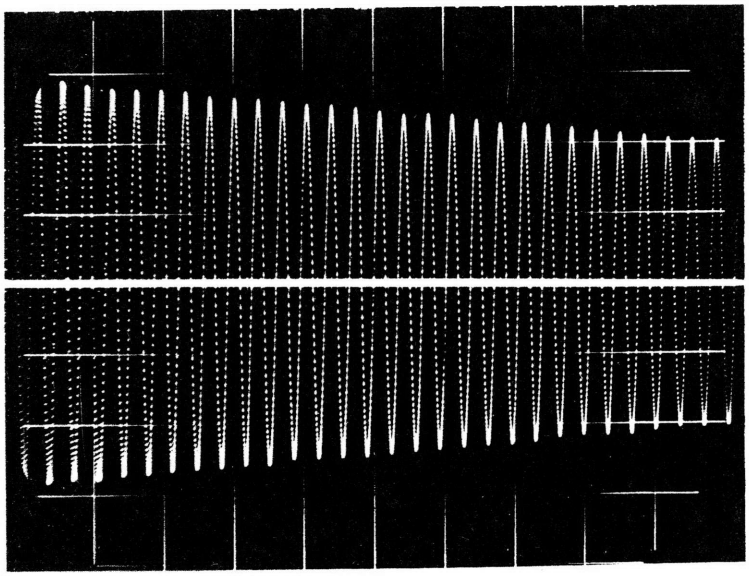

Fig. A-30

(Circular 0.015" 0.600 ata.)

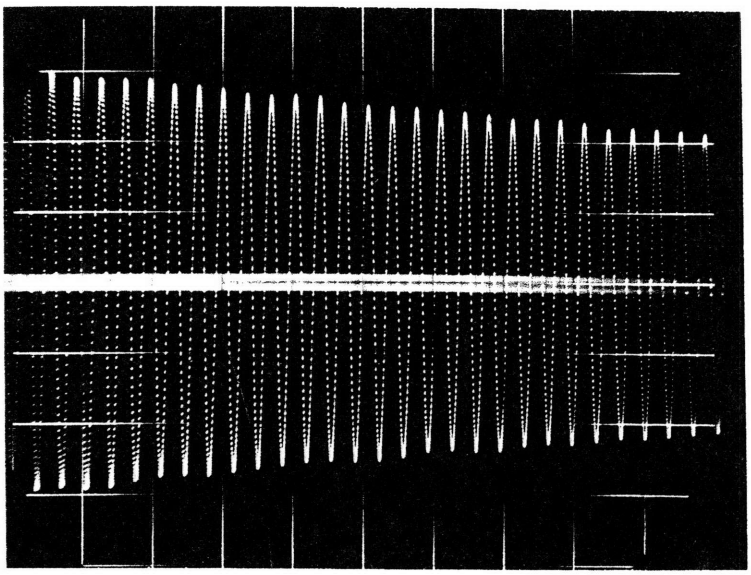

Fig. A- 31

(Circular o.o15" 0.330 ata.)

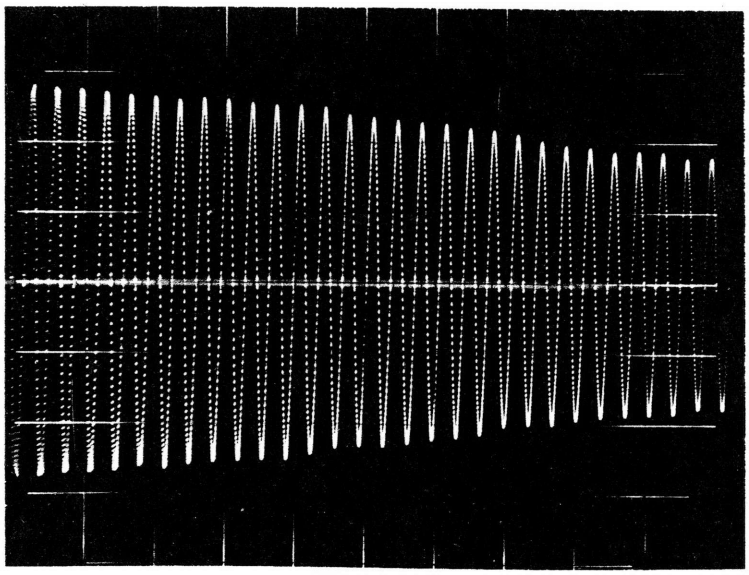

Fig. A-32

(Circular 0.015" 0.147 ata.)

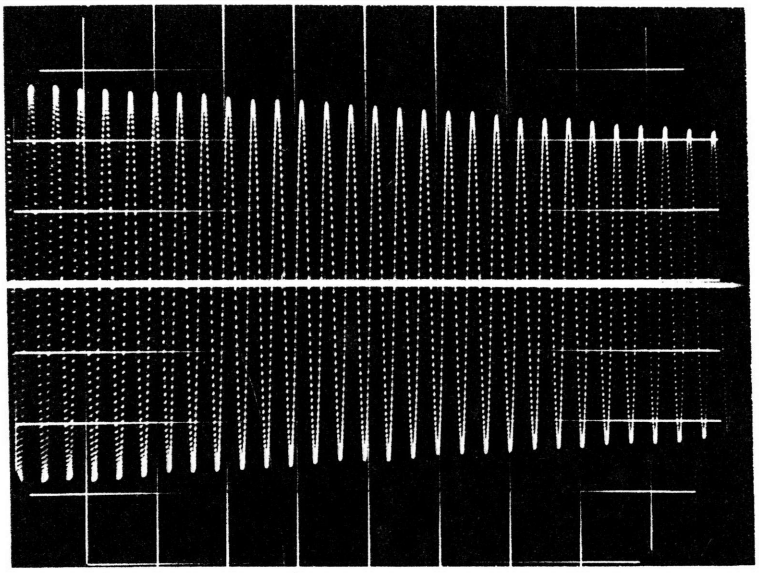

Fig. A-33

(Circular 0.020" 1 ata.)

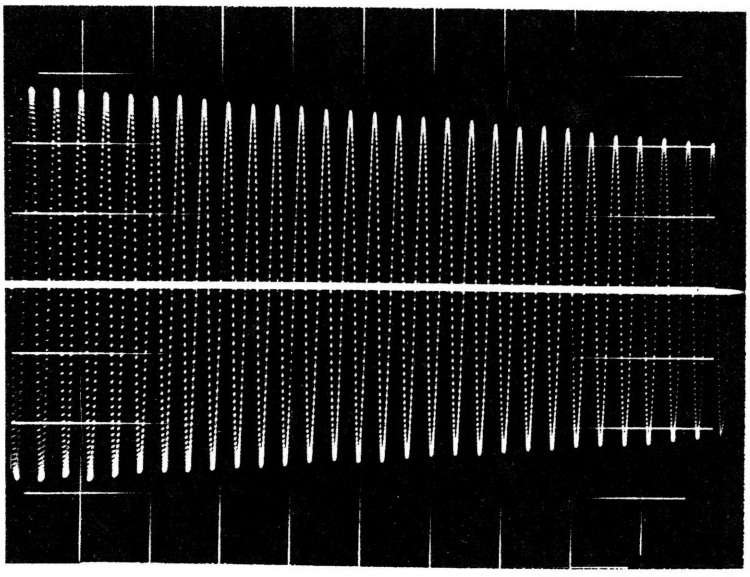

Fig. A-34

(Circular 0.020" 0.600 ata.)

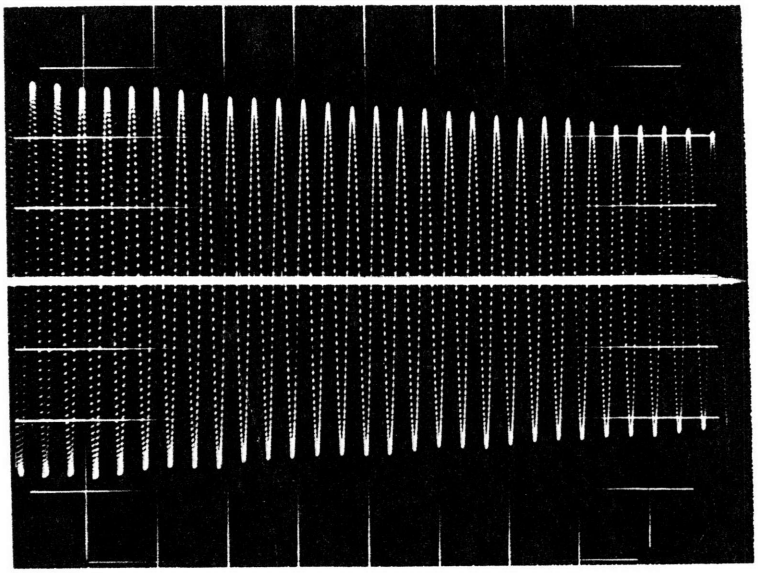

Fig. A-35

(Circular 0.020" 0.330 ata.)

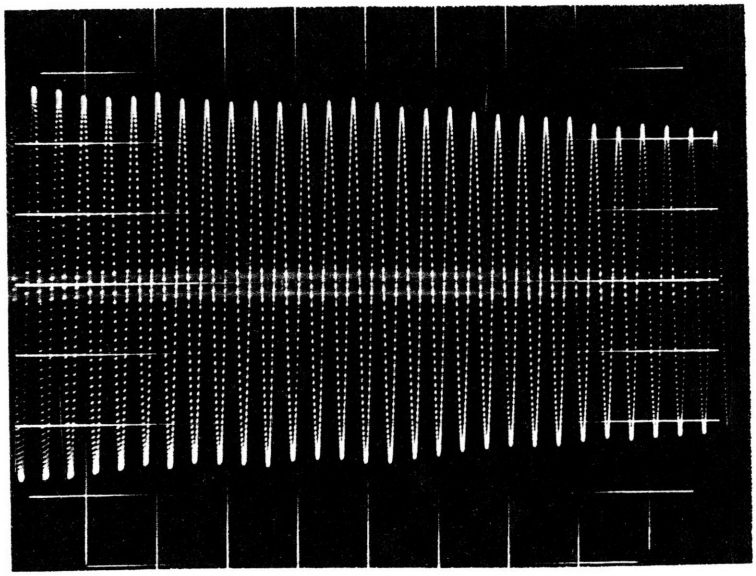

Fig. A- 36

(Circular 0.020" 0.147 ata.)

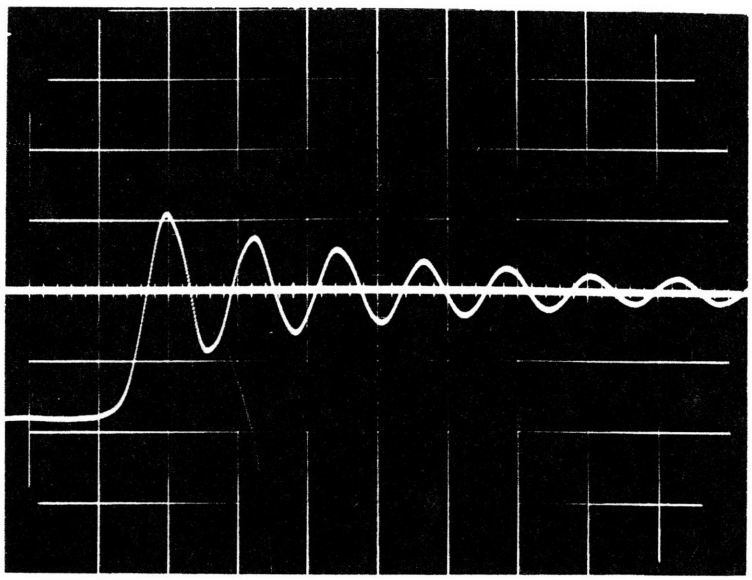

Fig. A-37

(Annular 0.001" 1 ata.)

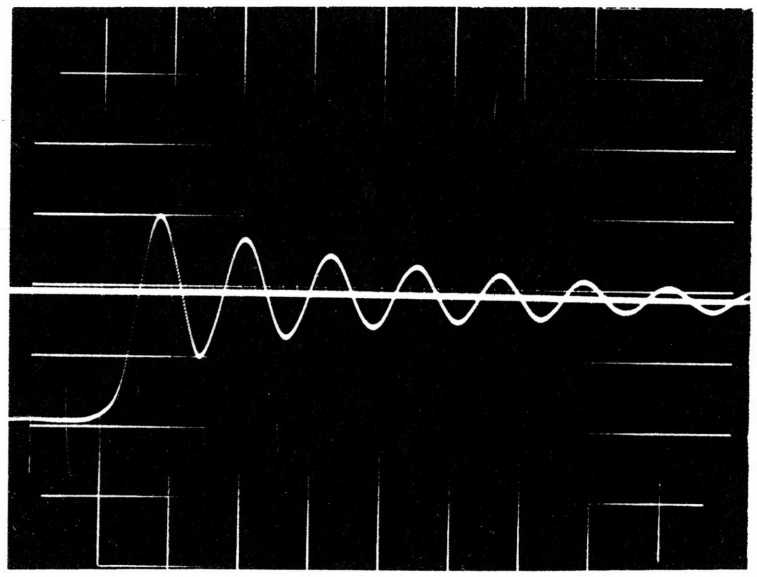

Fig. A-38

(Annular 0.001" 0.600 ata.)

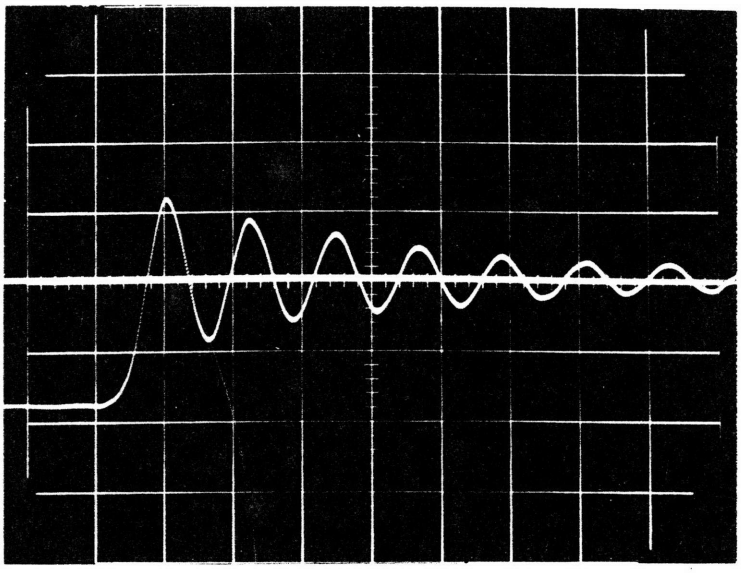

Fig. A-39

(Annular 0.001" 0.330 ata.)

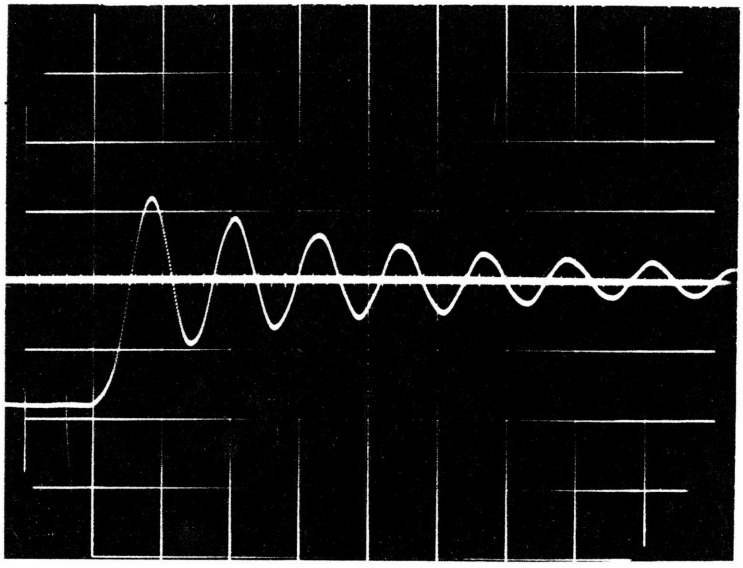

Fig. A-40

(Annular 0.001 0.147 ata.)

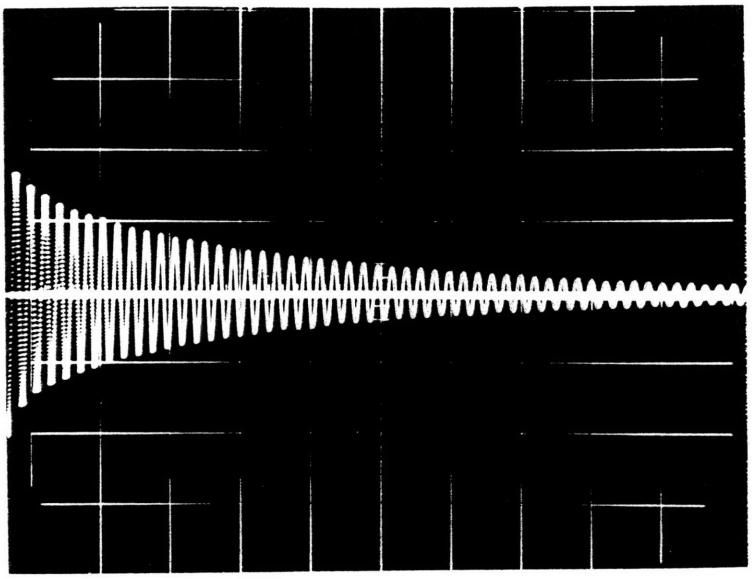

Fig. A-41

(Annular 0.002" 1 ata.)

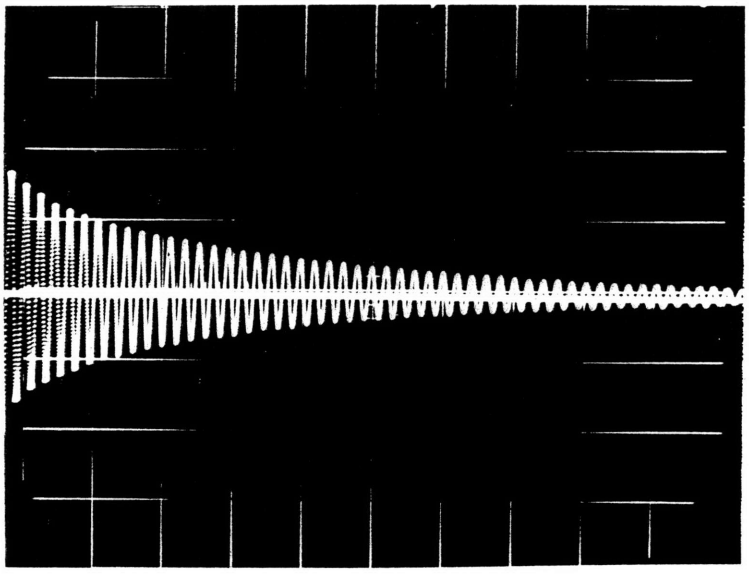

Fig. A-42

(Annular 0.002" 0.600 ata.)

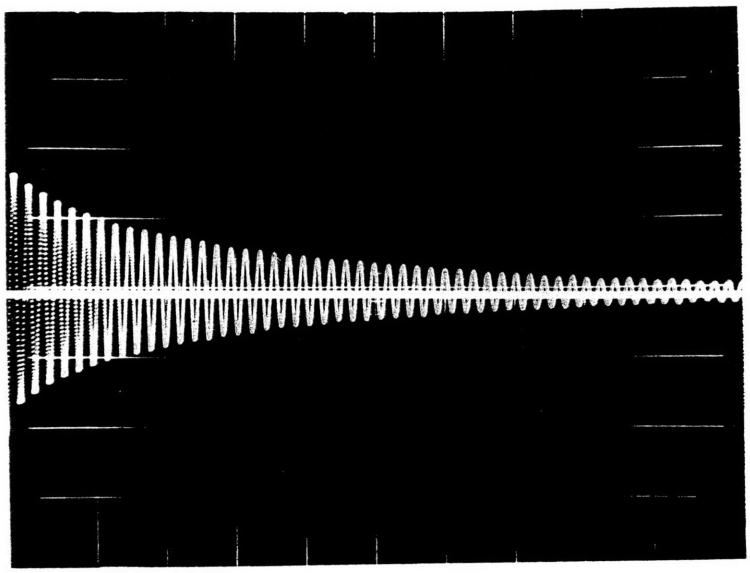

Fig. A-43

(Annular 0.002" 0.330 ata.)

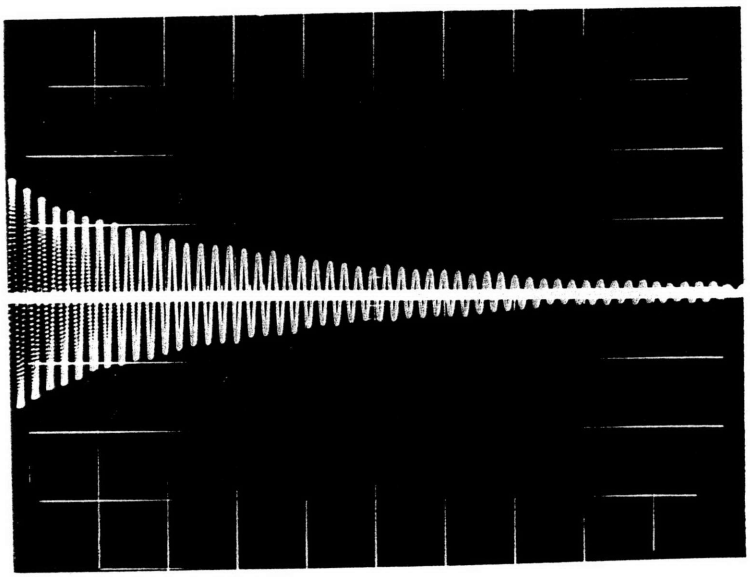

Fig. A-44

(Annular 0.002" 0.147 ata.)

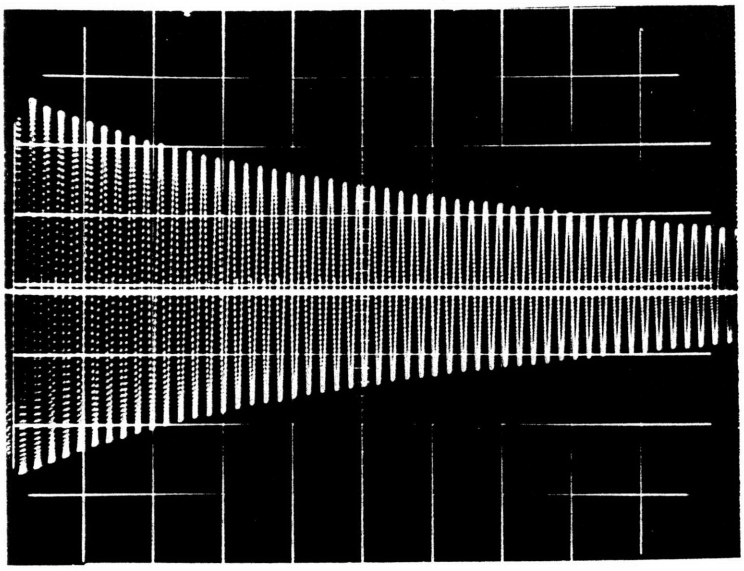

Fig. A-45

(Annular 0.003" 1 ata.)

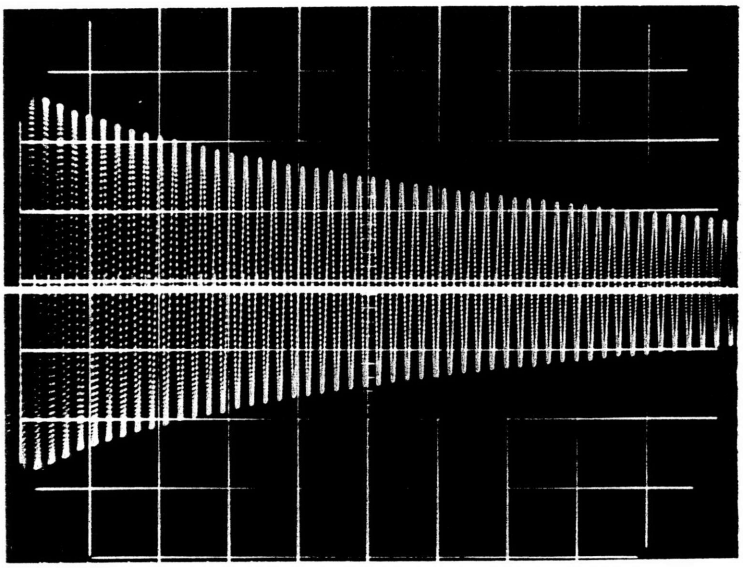

Fig. A-46

(Annular 0.003" 0.600 ata.)

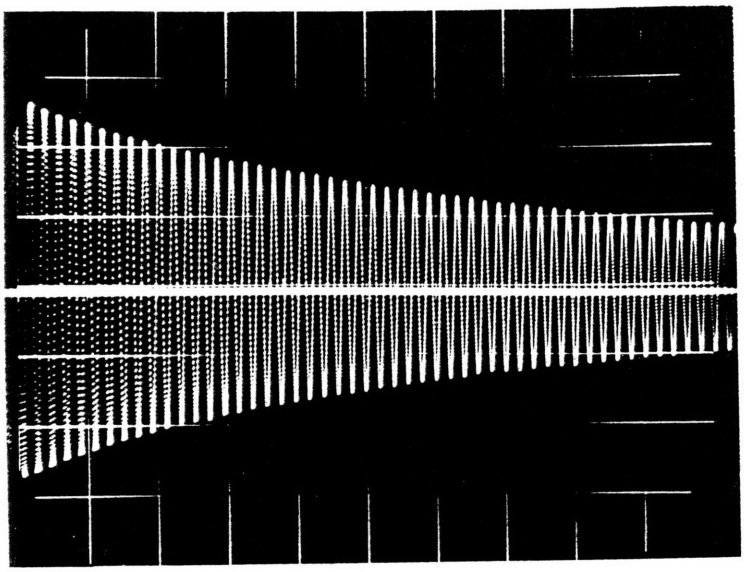

Fig. A-47

(Annular 0.003" 0.330 ata.)

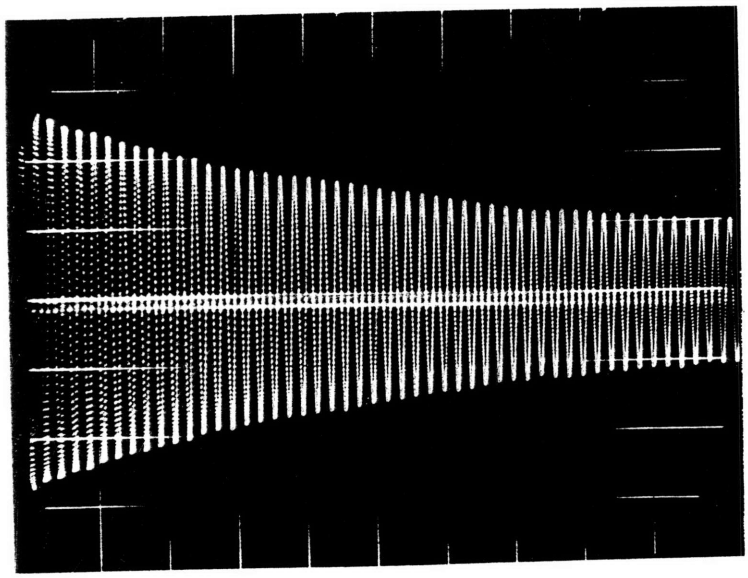

Fig. A-48

(Annular 0.003" 0.147 ata.)

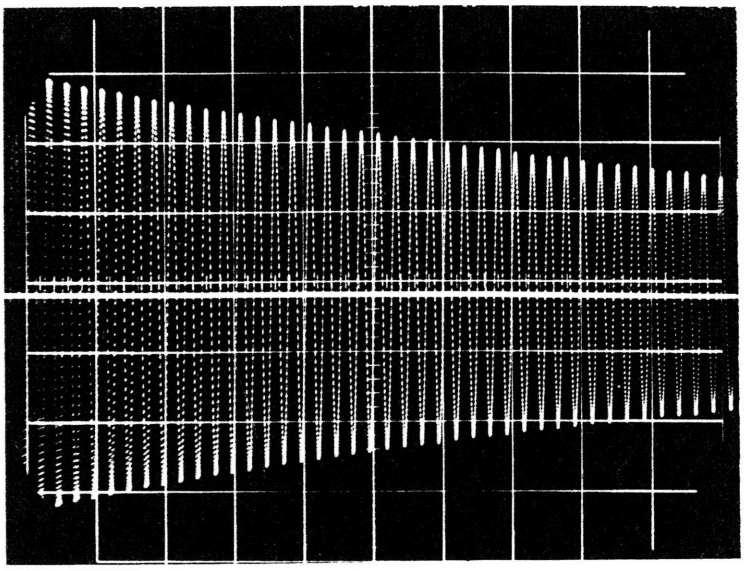

Fig. A-49

(Annular 0.004" 1 ata.)

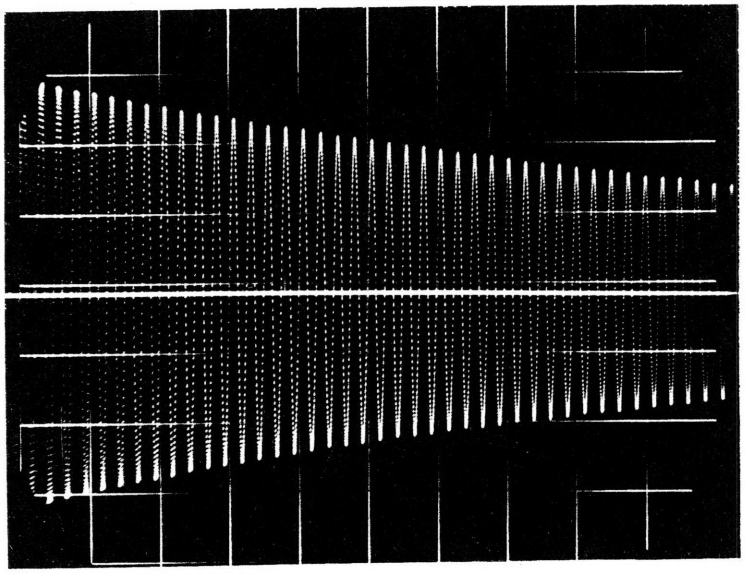

Fig. A-50

(Annular 0.004" 0.600 ata.)

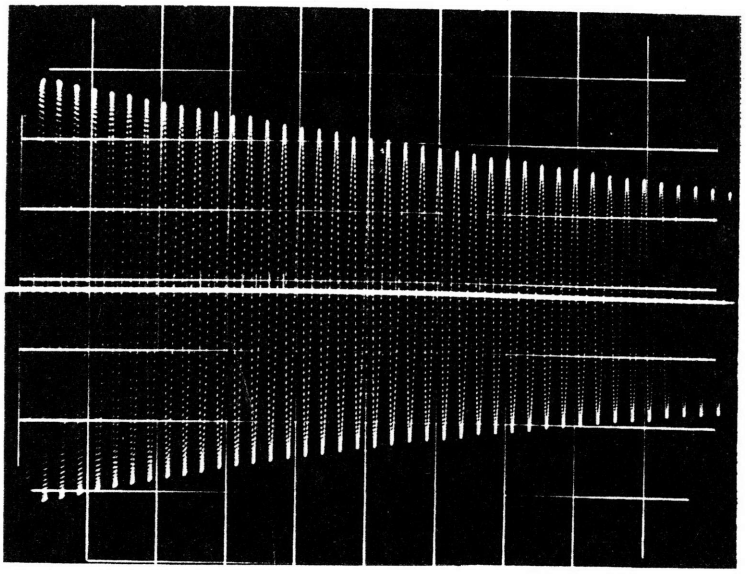

Fig. A-51

(Annular 0.004" 0.330 ata.)

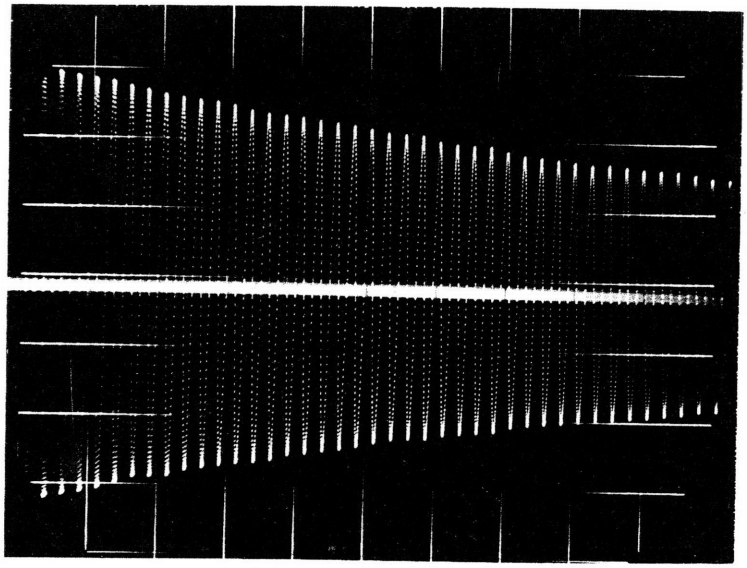

Fig. A-52

(Annular 0.004" 0.147 ata.)

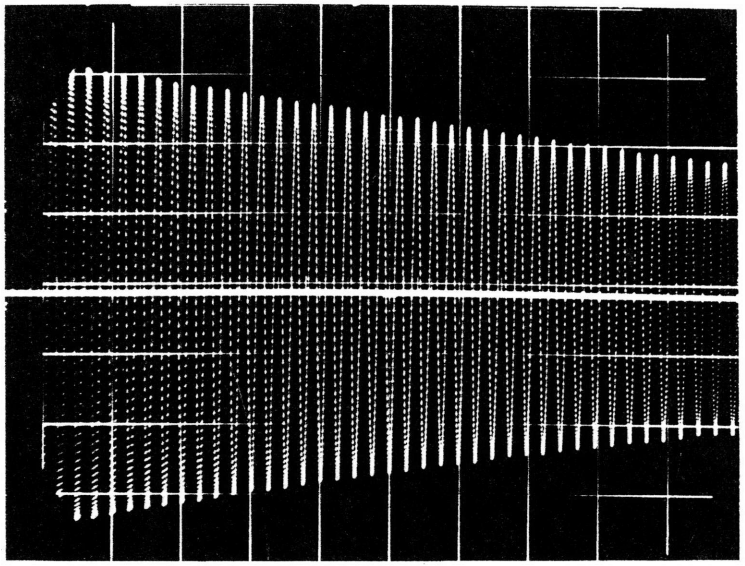

Fig. A-53

(Annular 0.005" 1 ata.)

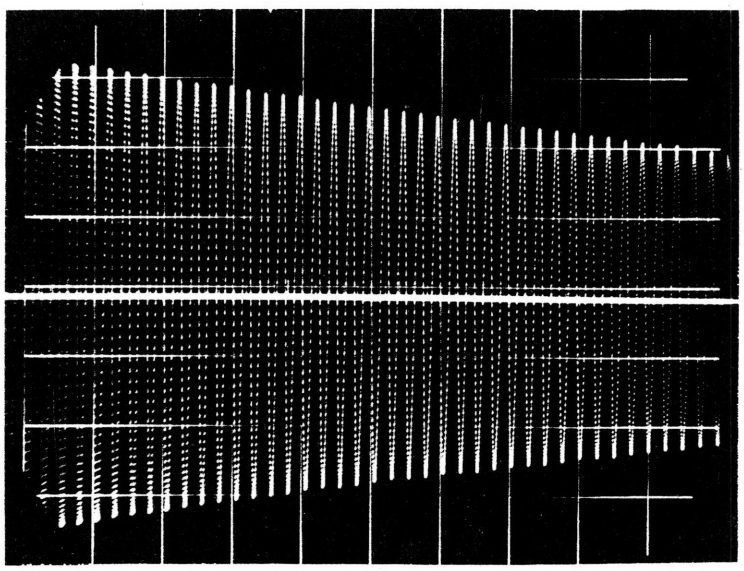

Fig. A-54

(Annular 0.005" 0.600 ata.)

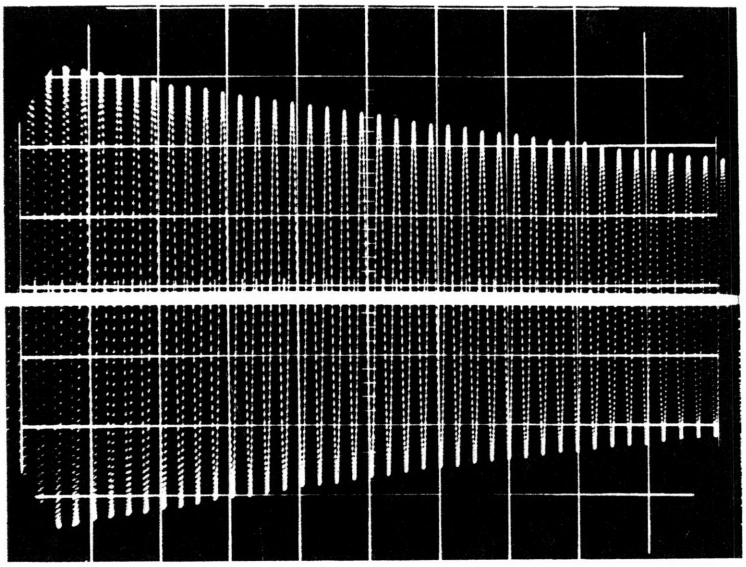

Fig. A-55

(Annular 0.005" 0.330 ata.)

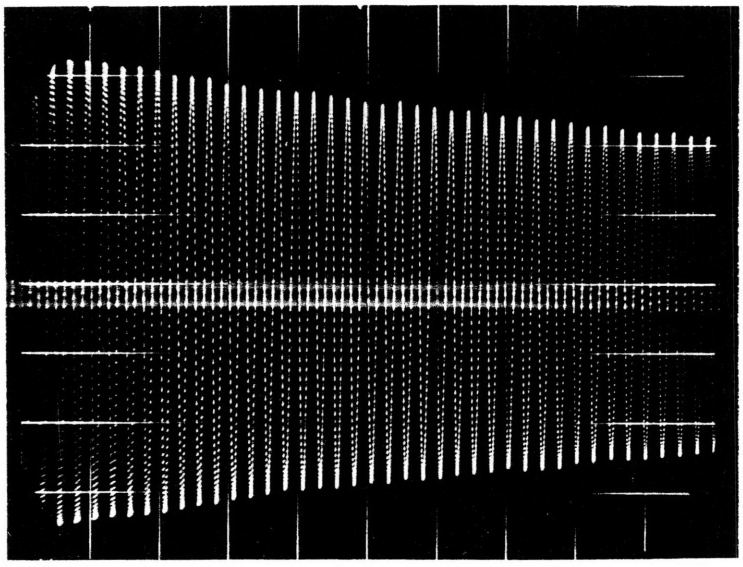

Fig. A-56

(Annular 0.005" 0.147 ata.)

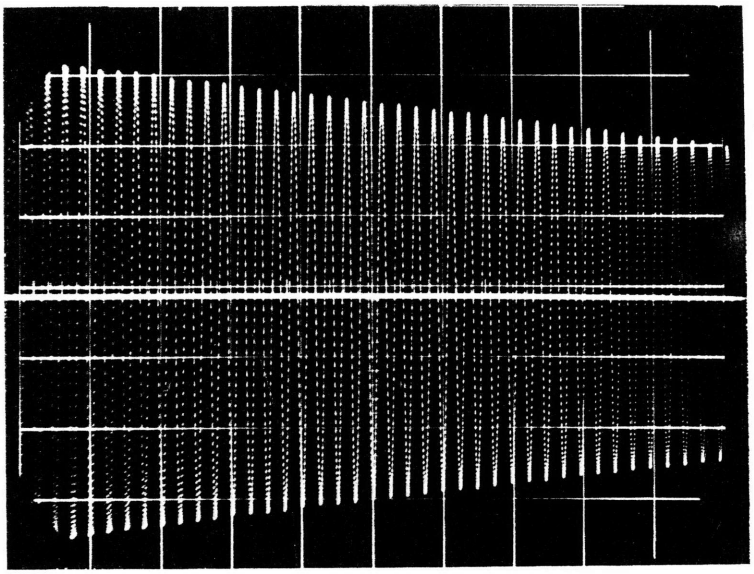

Fig. A-57

(Annular 0.007" 1 ata.)

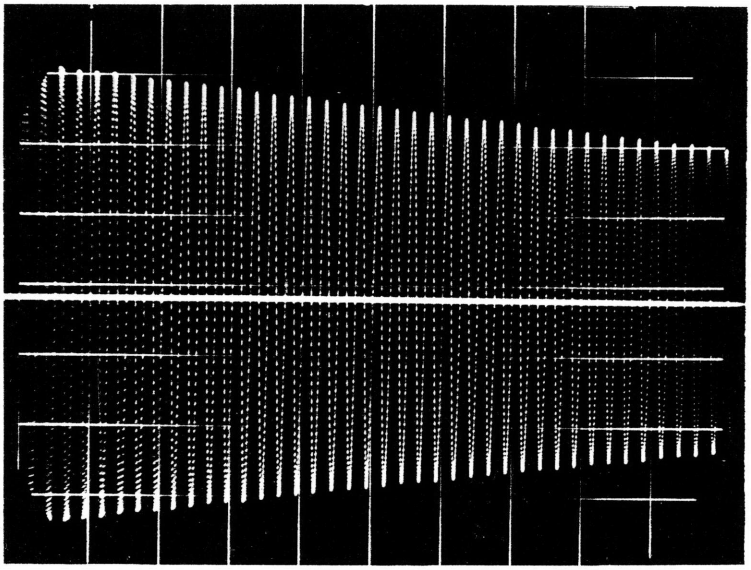

Fig. A-58

(Annular 0.007" 0.600 ata.)

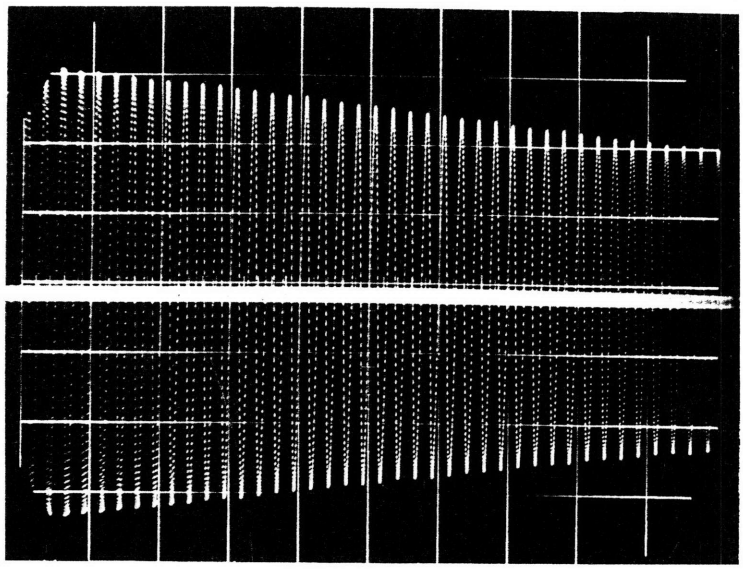

Fig. A-59

(Annular 0.007" 0.330 ata.)

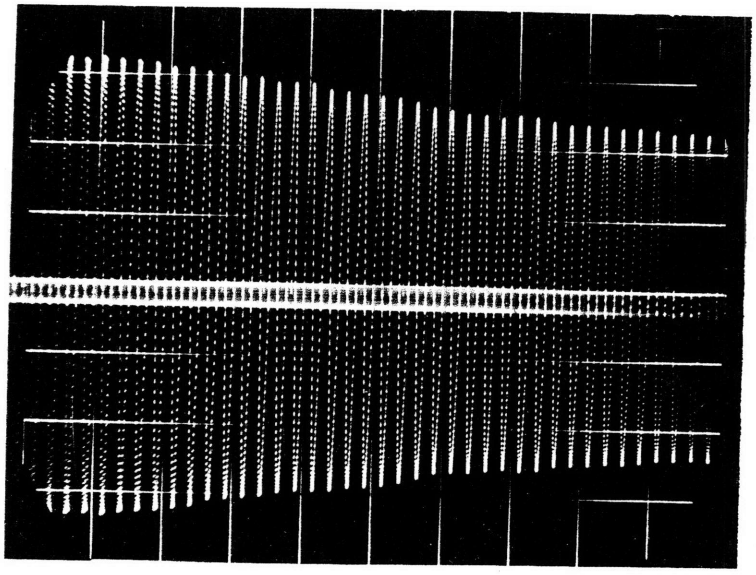

Fig. A-60

(Annular 0.007" 0.147 ata.)

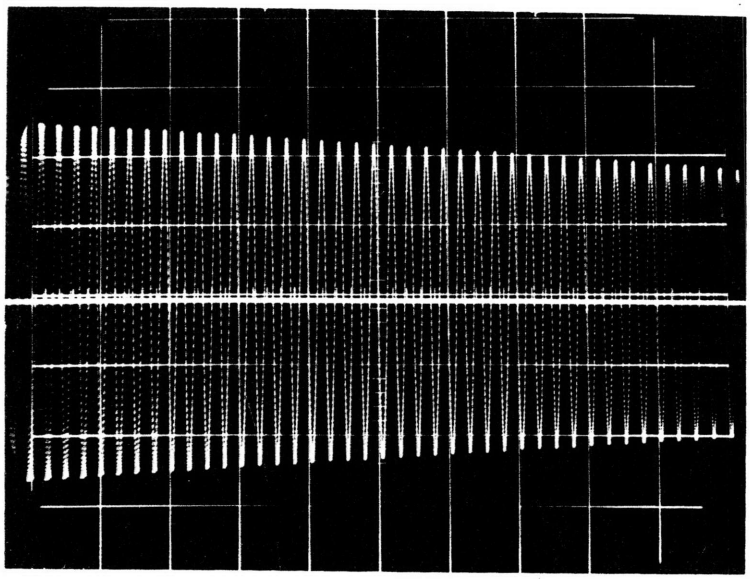

Fig. A-61

(Annular 0.010" 1 ata.)

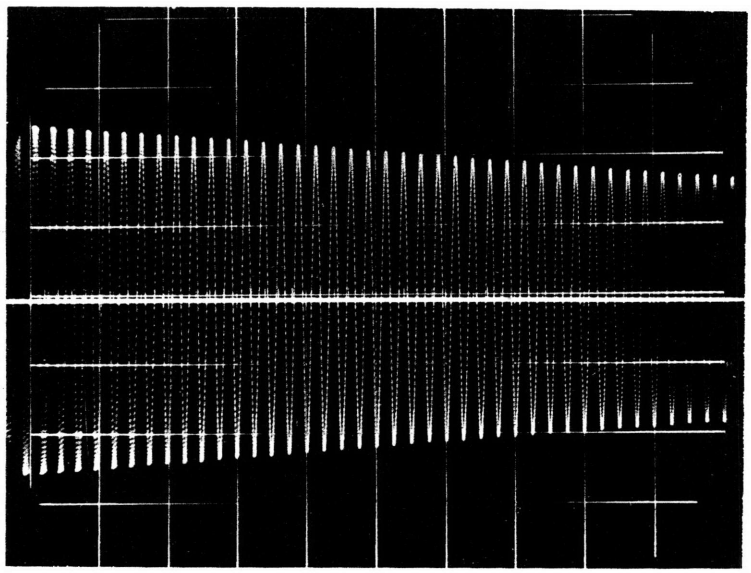

Fig. A-62

(Annular 0.010" 0.600 ata.)

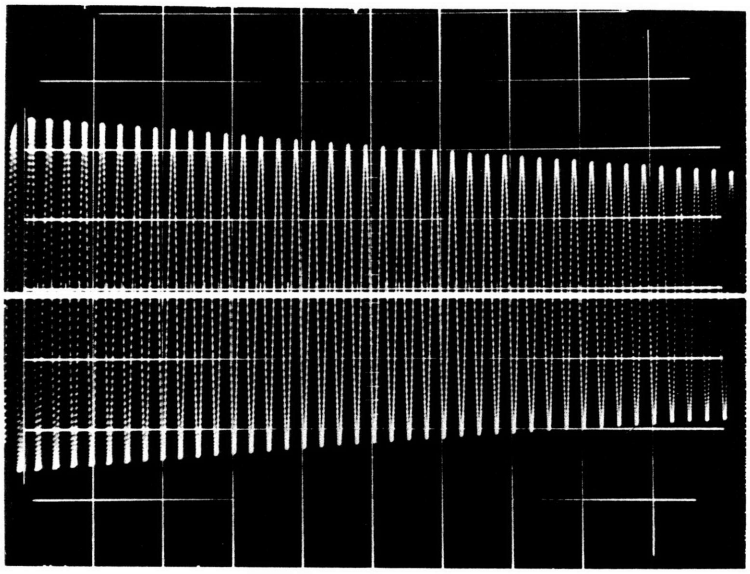

Fig. A-63

(Annular 0.010" 0.330 ata.)

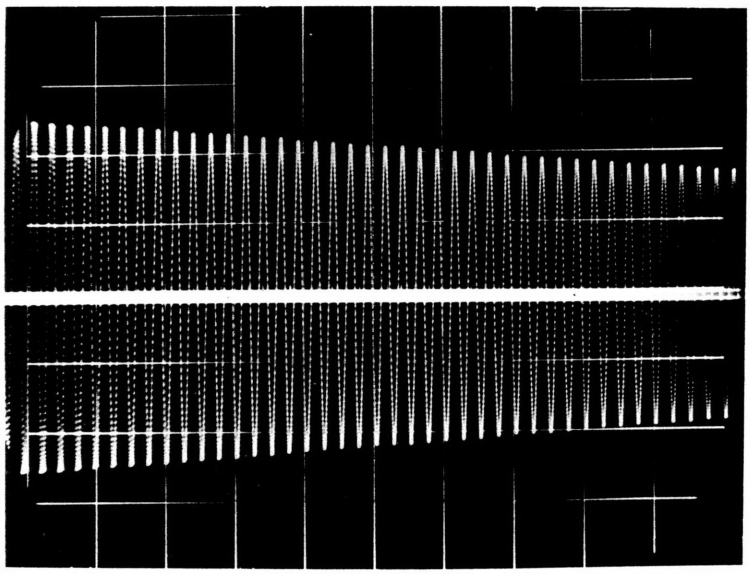

Fig. A-64

(Annular 0.010" 0.147 ata.)

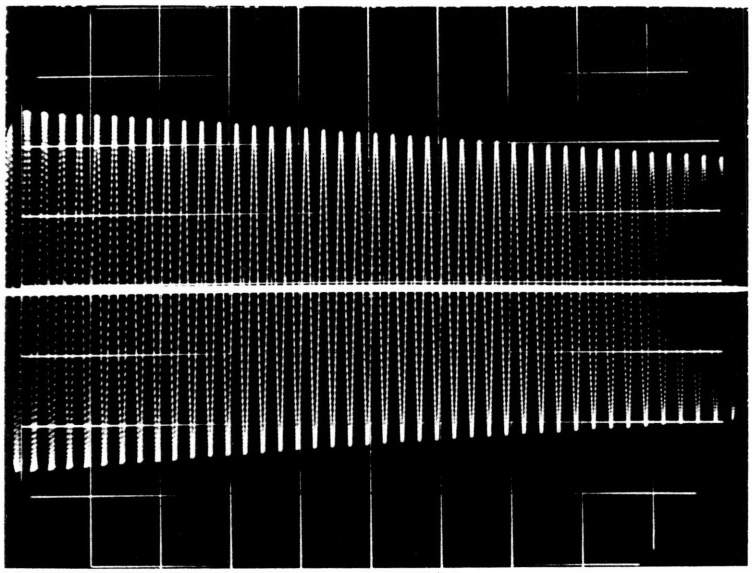

Fig. A-65

(Annular 0.015" 1 ata.)

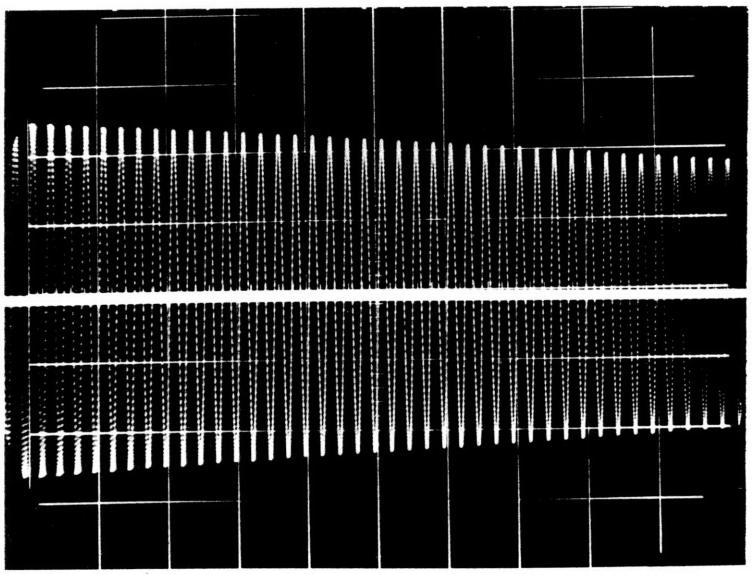

Fig. A-66

(Annular 0.015" 0.600 ata.)

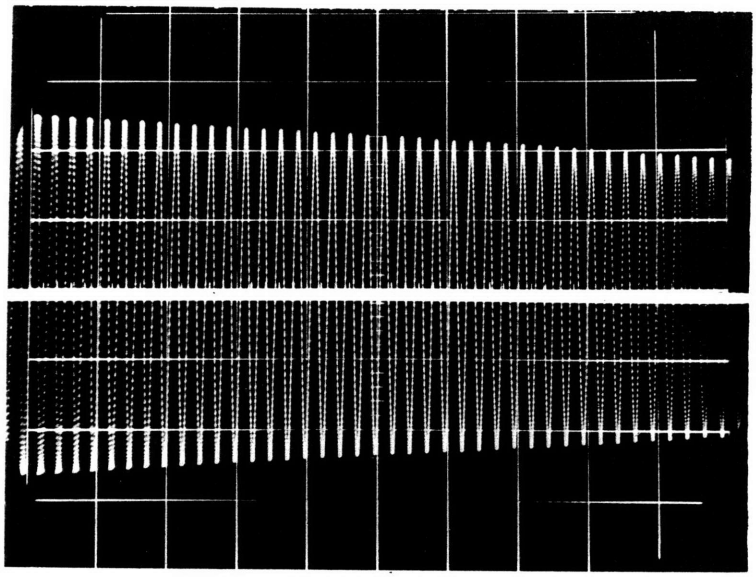

Fig. A-67

(Annular 0.015" 0.330 ata.)

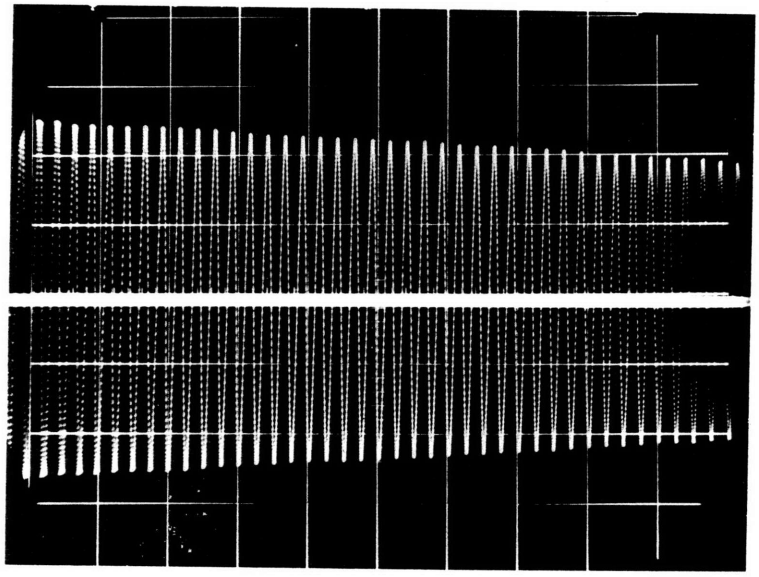

Fig. A-68

(Annular 0.015" 0.147 ata.)

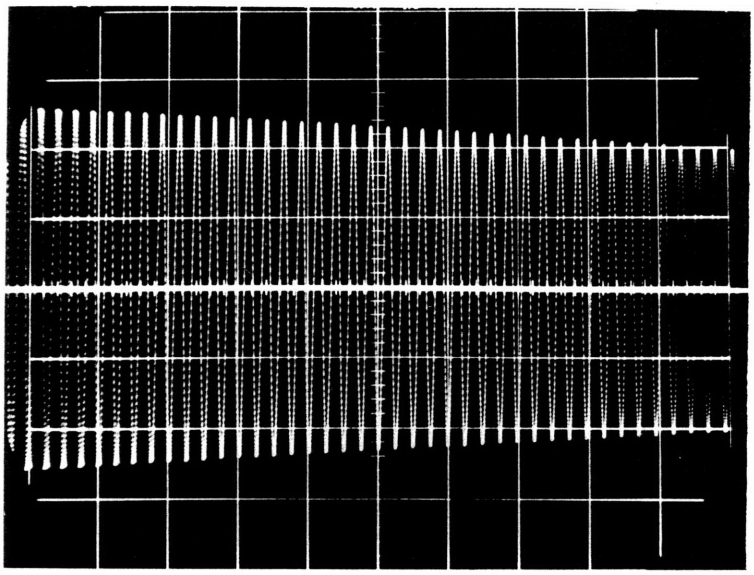

Fig. A-69

(Annular 0.020" 1 ata.)

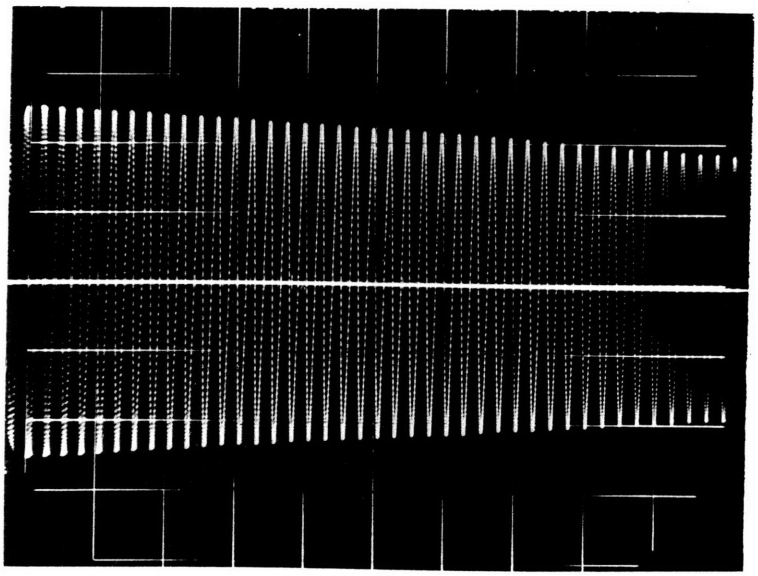

Fig. A-70

(Annular 0.020" 0.600 ata.)

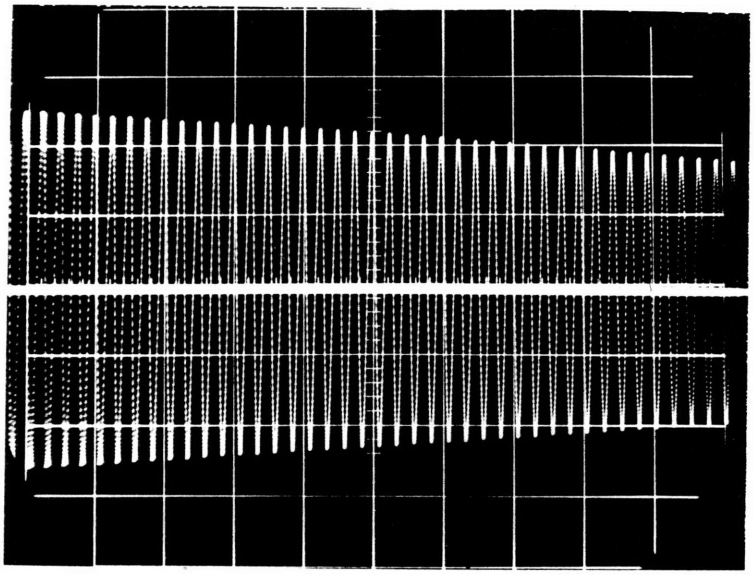

Fig. A-71

(Annular 0.020" 0.330 ata.)

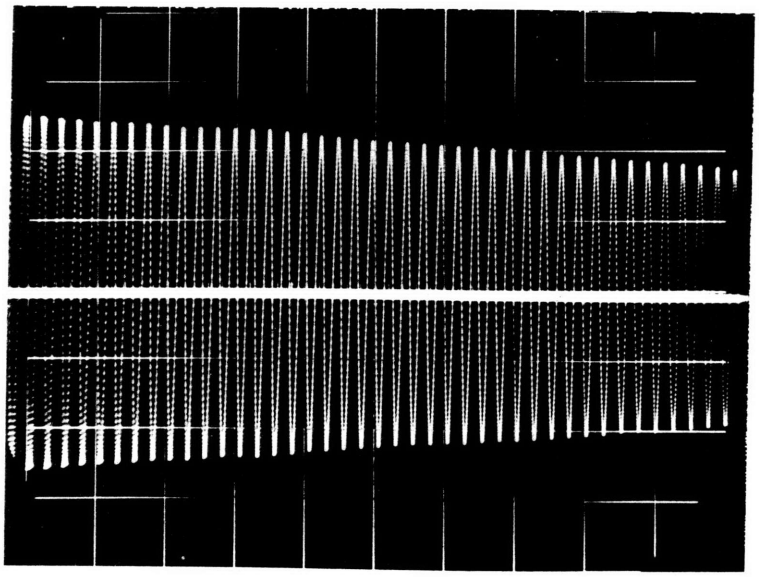

Fig. A-72

(Annular 0.020" 0.147 ata.)

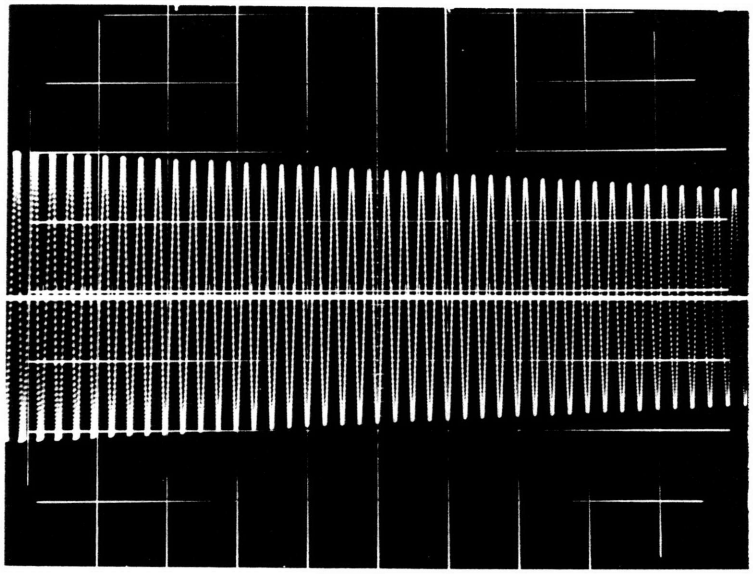

Fig. A-73

(Free oscillation 1 ata.)

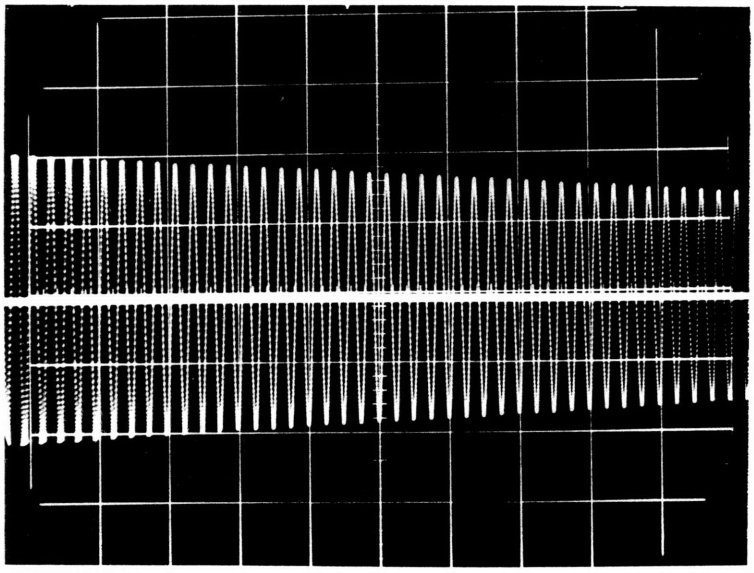

Fig. A-74

(Free oscillation 0.600 ata.)

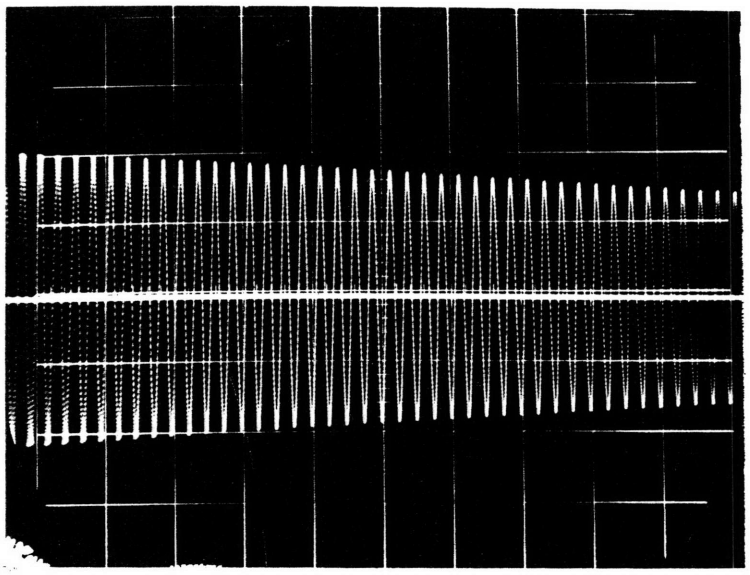

Fig. A-75

(Free oscillation 0.330 ata.)

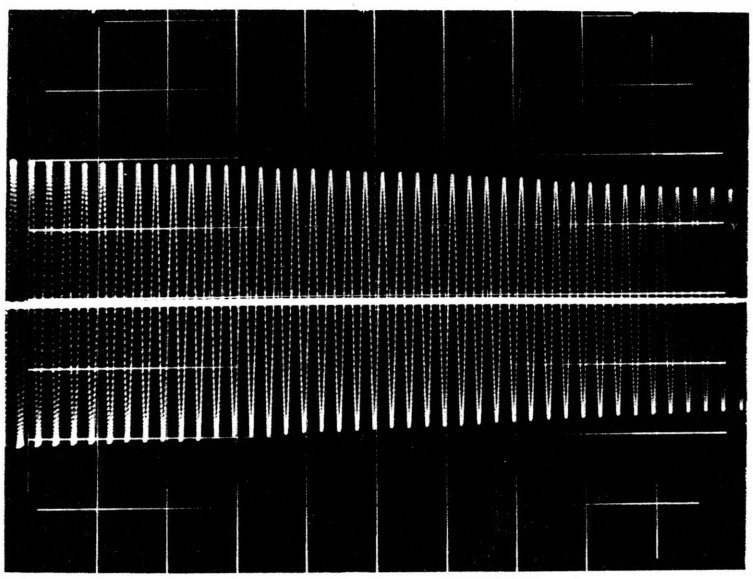

Fig. A-76

(Free oscillation 0.147 ata.)

References

1. Elrod, H.G. — A derivation of the basic equations for hydrodynamic lubrication with a fluid having constant properties. - Applied Mathematics (Jan. 1960.)

2. Langlois, W.E. — Isothermal Squeeze Films - IBM Research Report RJ-192 (May 22, 1961)

3. Michael, W.A. — Small Transient and Periodic Squeeze Motion in Parallel Gas Films - IBM Research Report RJ-197 (Sept. 25, 1961)

4. Jahnke and Emde, F. Funktionentafeln Dover Publication (1943)

5. Tables of Functions and of Zeros of Functions U.S. Department of Commerce National Bureau of Standards Applied Mathematics Series 37, 1954.

6. Chistova, E.A. — Tables of Bessel Functions of the true Argument and Integrals Derived from them Pergamon Press, Inc. 1959.

7. Schneider, P.J. — Conduction Heat Transfer Addison-Wesley Publication Company, Inc.

8. Carslaw, H.S., & Jasger, J.C. Conduction of Heat in Solids Oxford University Press 1959.

9. Crank, J. — Mathematics of Diffusion Oxford University Press 1957.

10. Gille, J.C. — Feedback Control Systems McGraw Hill Book Co., Inc. 1958

11. Savant, C.J. — Basic Feedback Control System Design McGraw Hill Book Co., Inc. 1958.

12. Prandtl, L. Essentials of Fluid Dynamics
Hafner Publishing Company 1952.

13. Lion, K.S. Instrumentation in Scientific Research
McGraw Hill Book Co., Inc. 1959

14. Keenan, J.H. & Kaye, J. Thermodynamic Properties of Air
John Wiley & Sons, Inc. 1945

15. Gray, A. Treatise on Bessel Functions and Their Applications to Physics
MacMillan & Co., Ltd. 1952.